bioRxiv preprint doi: https://doi.org/10.1101/180075; this version posted August 24, 2017. The copyright holder for this preprint (which was not certified by peer review) is the author/funder. All rights reserved. No reuse allowed without permission.

Evolutionary genetics of cytoplasmic incompatibility genes *cifA* and *cifB* in prophage WO of *Wolbachia*

Amelia R. I. Lindsey[1,7], Danny W. Rice[2], Sarah R. Bordenstein[3], Andrew W. Brooks[3,4], Seth R. Bordenstein*[3,4,5,6], Irene L. G. Newton*[2]

[1]Department of Entomology, University of California Riverside, Riverside, California, USA

[2]Department of Biology, Indiana University, Bloomington, Indiana, USA

[3]Department of Biological Sciences, Vanderbilt University, Nashville, Tennessee, USA

[4]Department of Pathology, Microbiology and Immunology, Vanderbilt University, Nashville, Tennessee, USA

[5]Vanderbilt Institute of Infection, Immunology, and Inflammation, Vanderbilt University, Nashville, Tennessee, USA

[6]Vanderbilt Genetics Institute, Vanderbilt University, Nashville, Tennessee, USA

[7]Current Address: Department of Biology, Indiana University, Bloomington, Indiana, USA

*Authors for Correspondence:

Irene L.G. Newton, Department of Biology, Indiana University, Bloomington, Indiana, USA, 812-855-3883, irnewton@indiana.edu, and Seth R. Bordenstein, Department of Biological Sciences, Vanderbilt University, Nashville, Tennessee, USA, 615-322-9087, s.bordenstein@vanderbilt.edu

bioRxiv preprint doi: https://doi.org/10.1101/180075; this version posted August 24, 2017. The copyright holder for this preprint (which was not certified by peer review) is the author/funder. All rights reserved. No reuse allowed without permission.

Abstract

The bacterial endosymbiont *Wolbachia* manipulates arthropod reproduction to facilitate its maternal spread through populations. The most common manipulation is cytoplasmic incompatibility (CI): *Wolbachia*-infected males produce modified sperm that cause embryonic mortality, unless rescued by eggs harboring the same *Wolbachia*. The genes underlying CI, *cifA* and *cifB,* were recently identified in the eukaryotic association module of *Wolbachia*'s prophage WO. Here, we use transcriptomic and genomic approaches to address three important evolutionary facets of these genes. First, we assess whether or not *cifA* and *cifB* comprise a classic toxin-antitoxin operon, and show they do not form an operon in strain *w*Mel. They coevolve but exhibit strikingly distinct expression across host development. Second, we provide new domain and functional predictions across homologs within *Wolbachia*, and we show amino acid sequences vary substantially across the genus. Lastly, we investigate conservation of *cifA* and *cifB* and find degradation and loss of the genes is common in strains that no longer induce CI. Taken together, we find no evidence for the operon hypothesis in *w*Mel, provide functional annotations that broaden the potential mechanisms of CI induction, illuminate recurrent erosion of *cifA* and *cifB* in non-CI strains, and advance an understanding of the most widespread form of reproductive parasitism.

Key words

symbiosis, reproductive manipulation, gene loss, bacteriophage

bioRxiv preprint doi: https://doi.org/10.1101/180075; this version posted August 24, 2017. The copyright holder for this preprint (which was not certified by peer review) is the author/funder. All rights reserved. No reuse allowed without permission.

Introduction

The genus *Wolbachia* is the most widespread group of maternally transmitted endosymbiotic bacteria (Zug and Hammerstein 2012). They occur worldwide in numerous arthropods and nematodes and can selfishly manipulate reproduction (Werren, et al. 2008), confer antiviral defense (Bian, et al. 2010; Teixeira, et al. 2008), and assist reproduction and development of their hosts (Dedeine, et al. 2001; Hoerauf, et al. 1999; Hosokawa, et al. 2010). The most common parasitic manipulation is cytoplasmic incompatibility (CI), whereby *Wolbachia*-infected males produce modified sperm that can only be rescued by eggs infected with the same *Wolbachia* strain (Yen and Barr 1971). If the modified sperm fertilize eggs infected with no *Wolbachia* (unidirectional CI) or a genetically-incompatible *Wolbachia* strain (bidirectional CI), then delayed histone deposition, improper chromosome condensation and cell division abnormalities result in embryonic mortality (Landmann, et al. 2009; Lassy and Karr 1996; Serbus, et al. 2008; Tram and Sullivan 2002). Other described reproductive manipulations include parthenogenesis (Stouthamer, et al. 1990), male-killing (Hurst, et al. 1999), and feminization (Rousset, et al. 1992), all of which give a fitness advantage to *Wolbachia*-infected females and thus assist the spread of the infected matriline through a population. These manipulations, once sustained, can also impact host evolution including speciation (Bordenstein, et al. 2001; Brucker and Bordenstein 2013; Jaenike, et al. 2006) and mating behaviors (Miller, et al. 2010; Moreau, et al. 2001; Randerson, et al. 2000; Shropshire and Bordenstein 2016).

In addition to the aforementioned reproductive manipulations, *Wolbachia* strains affect host biology by provisioning nutrients (Hosokawa, et al. 2010), altering host survivorship (Min and Benzer 1997) and fecundity (Dedeine, et al. 2001; Stouthamer and Luck 1993), and importantly,

bioRxiv preprint doi: https://doi.org/10.1101/180075; this version posted August 24, 2017. The copyright holder for this preprint (which was not certified by peer review) is the author/funder. All rights reserved. No reuse allowed without permission.

protecting the host against pathogens (Bian, et al. 2010; Hughes, et al. 2011; Kambris, et al. 2009; Moreira, et al. 2009; Teixeira, et al. 2008; Walker, et al. 2011). The combination of reproductive manipulations that enable *Wolbachia* to spread in a population, and the ability to reduce vector competence through pathogen protection, have placed *Wolbachia* in the forefront of efforts to control target arthropod populations (Bourtzis, et al. 2014; Hoffmann, et al. 2011; Turelli and Hoffmann 1991; Walker, et al. 2011; Zabalou, et al. 2004). Despite these important applications, the widespread prevalence of *Wolbachia* across arthropod taxa (Hilgenboecker, et al. 2008; Werren and Windsor 2000; Zug and Hammerstein 2012), and decades of research, only recently have the genes underlying CI been determined (Beckmann, et al. 2017; LePage, et al. 2017).

Two studies converged on the same central finding: coexpression of a pair of syntenic genes recapitulates the CI phenotype (Beckmann, et al. 2017; LePage, et al. 2017). Uninfected *Drosophila melanogaster* males transgencially expressing the two genes from *w*Mel *Wolbachia* caused CI-like embryonic lethality when crossed with uninfected females that was notably rescued by *w*Mel-infected females (LePage, et al. 2017). Additionally, the two *w*Mel genes separately enhanced *Wolbachia*-induced CI in a dose dependent manner when expressed in *Wolbachia*-infected males (LePage, et al. 2017). In a separate study, CI-like embryonic lethality was also recapitulated through transgenic coexpression in *D. melanogaster* males of homologous transgenes encoded by the *Wolbachia w*Pip strain (which infects *Culex* mosquitoes) (Beckmann, et al. 2017). These two genes occur in the recently discovered eukaryotic association module of temperate phage WO (Bordenstein and Bordenstein 2016), which was previously implicated in influencing CI (Bordenstein, et al. 2006; Duron, et al. 2006; Masui, et al. 2000; Sinkins, et al.

bioRxiv preprint doi: https://doi.org/10.1101/180075; this version posted August 24, 2017. The copyright holder for this preprint (which was not certified by peer review) is the author/funder. All rights reserved. No reuse allowed without permission.

2005). The presence of these genes within prophage WO has implications for the transmission of these genes, namely vertical transmission in the *Wolbachia* genome versus horizontal transfer of phage WO. The genes were proposed as candidate CI effectors due to the presence of one of the protein products in the spermathecae of infected female mosquitoes (Beckmann and Fallon 2013) and their absence in the *w*Au *Wolbachia* strain that lost CI function (Sutton, et al. 2014).

The *w*Mel homologs of these genes are designated cytoplasmic incompatibility factors *cifA* (locus WD0631) and *cifB* (locus WD0632), with *cifA* always encoded directly upstream of *cifB* (LePage, et al. 2017). The gene set occurrs in varying copy number across eleven total CI-inducing strains that correlates with CI levels. Core sequence changes of the two genes exhibit a pattern of codivergence and in turn closely match bidirectional incompatibility patterns between *Wolbachia* strains. Homologs of CifA and CifB protein sequences belong to four distinct phylogenetic types (designated Types I – IV) that do not correlate with various phylogenies of *Wolbachia* housekeeping genes or phage WO *gpW* (locus WD0640) (LePage, et al. 2017). The homologous sequences in *w*Pip also cluster in Type I, though they are 66% and 76% different from *w*Mel's, respectively (Beckmann, et al. 2017). Hereinafter we use *cifA* and *cifB* to refer to these genes, unless specifically referring to analyses of the *w*Pip homologs, *cidA* and *cidB*. *In vitro* functional analyses revealed that *cidB* can encode deubiquitylase activity, and *cidA* encodes a protein that binds CidB (Beckmann, et al. 2017). Mutating the catalytic residue in the deubiquitylating domain of CidB results in a loss of the CI-like function in transgenic flies (Beckmann, et al. 2017). Whether these genes have additional enzymatic or regulatory roles and which other residues are important for function remain open questions.

bioRxiv preprint doi: https://doi.org/10.1101/180075; this version posted August 24, 2017. The copyright holder for this preprint (which was not certified by peer review) is the author/funder. All rights reserved. No reuse allowed without permission.

There are important considerations for the location, organization, and characterization of these genes. Whether or not *cifA* and *cifB* form a strict, toxin-antitoxin operon is debatable, and likewise has important implications for how gene expression is regulated by *Wolbachia* during host infection. Support for the operon hypothesis is based on weak transcription across the junction between *cidA* and *cidB*, inferred to be due to the presence of polycistronic mRNA (Beckmann and Fallon 2013; Beckmann, et al. 2017); an alternative explanation is transcriptional slippage. Quantitative transcription analyses and computational predictions of operon structure do not support the operon hypothesis (LePage, et al. 2017). Moreover and importantly, transgenic studies show that both *cifA* and *cifB* are required for induction of CI and thus cannot form a strict toxin (*cifB*) - antitoxin (*cifA*) system. As both genes encode CI function and can individually enhance *Wolbachia*-induced CI, and there is mixed evidence for classification as an operon, it does not appear that characterization as a strict toxin-antitoxin operon is warranted (LePage, et al. 2017). However, like toxin-antitoxin systems, CidA binds CidB *in vitro* and expression of *cidA* rescues temperature-sensitive growth inhibition induced by *cidB* expression in *Saccharomyces*, via an as-yet-unknown mechanism (Beckmann, et al. 2017).

As it stands now, the genes remain largely unannotated with the exception of a few small domains. If other predicted protein domains occur in *cifA* and *cifB*, they would provide new hypotheses for the mechanism of CI. Finally, the sequence diversity and/or loss of *cif* genes across the *Wolbachia* tree may give insights into the selective conditions that maintain the *cif* genes versus those that do not. Exploration of *cif* gene regulation, expression, and function thus can provide a framework for more targeted investigations of *Wolbachia*-host interactions, and potentially inform the deployment of *Wolbachia*-based arthropod control.

bioRxiv preprint doi: https://doi.org/10.1101/180075; this version posted August 24, 2017. The copyright holder for this preprint (which was not certified by peer review) is the author/funder. All rights reserved. No reuse allowed without permission.

Materials and Methods

Expression

For analysis of RNAseq data we used our published approach (Gutzwiller, et al. 2015). Briefly, fastq sequences for 1 day old male and female flies were mapped against the *Wolbachia* *w*Mel reference genome (Ensembl Genomes Release 24, Wolbachia_endosymbiont_of_drosophila_melanogaster.GCA_000008025.1.24) using bwa mem v. 0.7.5a with default parameters in paired-end mode. Mapped reads were sorted and converted to BAM format using samtools v0.1.19 after which BAM files were used as input to Bedtools (bedcov) to generate pileups and count coverage at each position. For expression correlations between genes, the raw RNAseq counts were divided by (gene length + 99), where 99 corresponds to read length (100) – 1. Within a growth stage these values were multiplied by $1e^6$ / (sum of values in stage) (Li and Dewey 2011). A pairwise distance between all genes was defined as (1 – R), where the R is the Pearson correlation coefficient between the normalized expression values of two genes. Possible negative correlations would be "penalized" here, resulting in a larger distance. Distances were clustered using the Kitsch program of PHYLIP (Felsenstein 1989).

Operon Prediction *in silico*

We used the dynamic profile of the transcriptome above to identify operons within the *w*Mel genome using two different approaches. We used the program Rockhopper (McClure, et al. 2013), using default parameters, in conjunction with the BAM files generated above to delineate likely operons across the entire genome. In addition, we took a fine-scale approach, focusing on

bioRxiv preprint doi: https://doi.org/10.1101/180075; this version posted August 24, 2017. The copyright holder for this preprint (which was not certified by peer review) is the author/funder. All rights reserved. No reuse allowed without permission.

the junction between *cifA* and *cifB* (Fortino, et al. 2014), using the pileup files generated above and identifying drops in gene expression correlated to genomic position using a sliding window analysis.

Nucleic Acid Extractions and Quantitative PCR

To identify *Wolbachia* gene expression in adult male and female *D. melanogaster*, RNA was extracted from individual, age-matched flies (1-3 days old, stock 145) using a modified Trizol extraction protocol. Briefly, 500 uL of Trizol was added to individual flies and samples homogenized using a pestle. After a 5-minute incubation at room temperature, a 12,000 rcf centrifugation (at 4C for 10 min) was followed by a chloroform extraction. Aqueous phase containing RNA was extracted a second time with phenol:chloroform before isopropanol precipitation of RNA. This RNA pellet was washed and resuspended in THE RNA Storage Solution (Ambion). To detect the number of *cifA* and *cifB* transcripts as well as RNA levels across the junction between *cifA* and *cifB,* we utilized the RNA extracted from these flies and the SensiFAST SYBER Hi-ROX One-step RT mix (Bioline) and the Applied Biosystems StepOne Real-time PCR system with the following primer sets: *cifAF*: ATAAAGGCGTTTCAGCAGGA, *cifAR*: TCAATGAGGCGCTTCTAGGT; *cifBF*: TACGGGAAGTTTCATGCACA, *cifBR*:TTGCCAGCCATCATTCATAA; *cifA*_endF: TCTGGTTCTCATAAGAAAAGAAGAATC, *cifB*_begR: AACCATCAAGATCTCCATCCA. As a reference for transcription activity of the core *Wolbachia* genome, we utilized the *Wolbachia ftsZ* gene (Forward: TTTTGTTGTCGCAAATACCG; Reverse: AGCAAAGCGTTCACATTTCC). We designed primers to *ftsZ* because as a core protein involved in cell division, the quantities of *ftsZ* would better correlate with bacterial numbers and

bioRxiv preprint doi: https://doi.org/10.1101/180075; this version posted August 24, 2017. The copyright holder for this preprint (which was not certified by peer review) is the author/funder. All rights reserved. No reuse allowed without permission.

activity. Reactions were performed in duplicate or triplicate in a 96-well plate and CT values generated by the machine, were used to calculate the relative amounts of *Wolbachia* using the ΔΔCt (Livak) method.

Correlated Cif Trees and Distance Matrices

Quantifying congruence scores between the CifA and CifB trees was carried out with Matching Cluster (MC) and Robinson Foulds (RF) metrics using a custom python script previously described (Brooks, et al. 2016) and the TreeCmp program (Bogdanowicz, et al. 2012). MC weights topological congruency of trees, similar to the widely used RF metric. However, MC takes into account sections of subtree congruence and therefore is a more refined evaluation of small topological changes that affect incongruence. Significance in the MC and RF analyses was determined by the probability of 100,000 randomized bifurcating dendrogram topologies yielding equivalent or more congruent trees than the actual tree. Normalized scores were calculated as the MC and RF congruency score of the two topologies divided by the maximum congruency score obtained from random topologies. The number of trees that had an equivalent or better score than the actual tree was used to calculate the significance of observing that topology. Mantel tests were also performed on the CifA and CifB patristic distance matrices calculated in Geneious v8.1.9 (Kearse, et al. 2012). A custom Jupyter notebook (Pérez and Granger 2007) running python v3.5.2 (http://python.org) was written in the QIIME2 (Caporaso, et al. 2010) anaconda environment, and the Mantel test (Mantel 1967) utilized the scikit-bio v0.5.1 (scikit-bio.org) Mantel function run using scikit-bio distance matrix objects for each gene. The Mantel test was run with 100,000 permutations to calculate significance of the Pearson correlation coefficient between the two matrices using a two-sided correlation hypothesis.

bioRxiv preprint doi: https://doi.org/10.1101/180075; this version posted August 24, 2017. The copyright holder for this preprint (which was not certified by peer review) is the author/funder. All rights reserved. No reuse allowed without permission.

206

207 **Genomes Used in Comparative Analyses**

208 In order to identify *cif* homologs across the *Wolbachia* genomes, we defined orthologs across
209 existing, sequenced genomes using reciprocal best blastp. We included *Wolbachia* genomes
210 across five Supergroups: monophyletic clades of *Wolbachia* based on housekeeping genes,
211 denoted by uppercase letters (O'Neill, et al. 1992; Werren, et al. 1995). Supergroups A and B are
212 the major arthropod infecting lineages, while C and D infect nematodes (Bandi, et al. 1998).
213 Supergroup F *Wolbachia* infect a variety of hosts (Lo, et al. 2002). Included in this analysis were
214 11 type A strains (*w*Ri, *w*Ana, wSuzi, *w*Ha, *w*Mel, *w*MelPop, *w*Au, *w*Rec, *w*Gmm, *w*Uni,
215 *w*VitA), 10 type B strains (*w*PipJHB, *w*PipPel, *w*PipMol, *w*Bol1-b, *w*Bru, *w*CauB, *w*No, *w*Tpre,
216 *w*AlbB, *w*Di), 2 type C strains (*w*Ov, *w*Oo), and one each type D (*w*Bm) and type F (*w*Cle). We
217 included all genomic data available for each strain such that if multiple assemblies existed for
218 each *Wolbachia* variant (such as in the case of *w*Uni) we included the union of all available
219 contigs for that strain. *Wolbachia* orthologs were defined based on reciprocal best blast hits
220 between amino acid sequences in *Wolbachia* genomes. An orthologous group of genes was
221 defined by complete linkage such that all members of the group had to be the reciprocal best hit
222 of all other members of the group. *w*Ana, *w*Gmm, *w*PipMol, *w*Bru, and *w*CauB were not used in
223 subsequent analyses due to problematic assemblies. Information on strain phenotypes, hosts, and
224 accession numbers can be found in Table 1.

225

226 **Cif Phylogenetics**

227 CifA and CifB protein sequences were identified using BLASTp searches of WOMelB WD0631
228 (NCBI accession number AAS14330.1) and WD0632 (AAS14331.1), respectively. Homologs

bioRxiv preprint doi: https://doi.org/10.1101/180075; this version posted August 24, 2017. The copyright holder for this preprint (which was not certified by peer review) is the author/funder. All rights reserved. No reuse allowed without permission.

were selected based on: 1) $E = \leq 10^{-30}$, 2) query coverage greater than 70%, and 3) presence in fully sequenced *Wolbachia* genomes. All sequences were intact with the exception of a partial WOSuziC CifA (WP_044471252.1) protein. The missing N-terminus was translated from the end of contig accession number CAOU02000024.1 and concatenated with partial protein WP_044471252.1 for analyses, resulting in 100% amino acid identity to WORiC CifA (WP_012673228.1). In addition, two previously identified sequences (LePage, et al. 2017), WORecB CifB and WORiB CifB, were not available in NCBI's database and translated from nucleotide accession numbers JQAM01000018.1 and CP001391.1, respectively. The previously identified WOSol homologs (CifA: AGK87106 and CifB: AGK87078) (LePage, et al. 2017) were also included in our analyses. All protein sequences were aligned with the MUSCLE (Edgar 2004) plugin in Geneious Pro version 8.1.7 (Kearse, et al. 2012); the best models of evolution, according to corrected Akaike (Hurvich and Tsai 1993) information criteria, were estimated to be JTT-G using the ProtTest server (Abascal, et al. 2005); and phylogenetic trees were built using the MrBayes (Ronquist, et al. 2012) plugin in Geneious.

Protein Structure

All candidate CI gene protein sequences were assessed for the presence of domain structure using HHpred (https://toolkit.tuebingen.mpg.de/hhpred/ (Söding, et al. 2005)) with default parameters and the following databases: SCOPe95_2.06, SCOPe70_2.06, cdd_04Jul16, pfamA_30.0, smart_04Jul16, COG_04Jul16, KOG_04_Jul16, pfam_04Jul16, and cd_04Jul16. Schematics were created in inkscape (https://inkscape.org/), to show regions with significant structural hits, at a corrected p-value of $p < 0.05$. Modules were defined based on the presence of multiple highly significant hits within a region.

bioRxiv preprint doi: https://doi.org/10.1101/180075; this version posted August 24, 2017. The copyright holder for this preprint (which was not certified by peer review) is the author/funder. All rights reserved. No reuse allowed without permission.

252

253 **Protein Conservation**

254 Protein conservation was determined with the Protein Residue Conservation Prediction tool
255 (http://compbio.cs.princeton.edu/conservation/index.html (Capra and Singh 2007)), using
256 aligned amino acid sequences, Shannon entropy scores, a window size of zero, and sequence
257 weighting set to "false". Conservation was subsequently plotted in R version 3.3.2, and module
258 regions were delineated according to coordinates of the WOMelB modules within the alignment.
259 CI gene conservation scores were calculated separately for Type I sequences, and for all types
260 together. For CifB Type I sequences, the WOVitA4 ortholog was left out, due to the extended C-
261 terminus of that protein. Conservation scores were also calculated for "control proteins": Wsp
262 (*Wolbachia* surface protein), known to be affected by frequent recombination events (Baldo, et
263 al. 2005), and FtsZ, which is relatively unaffected by recombination (Baldo, et al. 2006b; Ros, et
264 al. 2009). Variation in amino acid conservation between modules and non-module regions was
265 assessed in R version 3.3.2 with a one-way ANOVA including "region" (either the unique
266 module number, or "non-module") as a fixed effect, and followed by Tukey Honest Significant
267 Difference for post hoc testing.

268

269 **Cif Modules**

270 The WOMelB structural regions delineated by HHpred were used to search for the presence of
271 Cifs or remnants of Cifs across the *Wolbachia* phylogeny. Amino acid sequences of the
272 WOMelB modules were queried against complete genome sequences (Table 1) using tblastn.
273 Any hit that was at least 50% of the length and 30% identity, or at least 90% of the length and
274 20% identity of the WOMelB module was considered a positive match. Module presence was

bioRxiv preprint doi: https://doi.org/10.1101/180075; this version posted August 24, 2017. The copyright holder for this preprint (which was not certified by peer review) is the author/funder. All rights reserved. No reuse allowed without permission.

plotted across a *Wolbachia* phylogeny constructed using the five Multi Locus Sequence Typing (MLST) genes defined by Baldo *et al.* (Baldo, et al. 2006b). Nucleotide sequences were aligned with MAFFT version 7.271 (Katoh and Standley 2013), and concatenated prior to phylogenetic reconstruction with RAxML version 8.2.8 (Stamatakis 2014), the GTRGAMMA substitution model, and 1000 bootstrap replicates.

Hidden Markov Model Searches

To identify *cif* homologs in draft *Wolbachia* genome assemblies we used the program suite HMMER (Eddy 2011). We defined *cif* types based on our phylogenetic trees (Figure 4) and used aligned amino acids from these types as input to HMMBUILD, using default parameters. We then searched six *Wolbachia* WGS assemblies (NCBI project numbers PRJNA310358, PRJNA279175, PRJNA322628) using HMMSEARCH with –F3 1e-20 –cut_nc and –domE 1e-10. Regardless of thresholds used, or *cif* type of HMM, resulting hits did not differ.

Results

***cifA* and *cifB* are Not Co-transcribed or Co-regulated and Do Not Comprise an Operon in *w*Mel**

To assess the operon hypothesis, we reasoned that genes which are co-transcribed and co-regulated will exhibit the following properties: similar total expression levels in whole animals and correlated gene expression across host development. We therefore utilized an existing RNAseq dataset for *Wolbachia* in *Drosophila melanogaster*, covering 24 life cycle stages and 3 time samplings each for adult males and females (Gutzwiller, et al. 2015). We mapped reads to the existing *w*Mel assembly (see methods), and calculated Pearson correlation coefficients for

bioRxiv preprint doi: https://doi.org/10.1101/180075; this version posted August 24, 2017. The copyright holder for this preprint (which was not certified by peer review) is the author/funder. All rights reserved. No reuse allowed without permission.

298 normalized expression values for each pairwise comparison across host development. In adult
299 males and females, *cifA* and *cifB* in *w*Mel are not expressed at similar levels (Figure 1), with *cifA*
300 expressed at significantly higher levels compared to *cifB* (eight-fold higher based on RPKM
301 values across both genes).
302
303 To further explore expression of the *cif* genes in *w*Mel and assess whether or not polycistronic
304 mRNA is produced, we performed a quantitative PCR analysis of gene expression from three-
305 day old male and female flies (Figure 2). We observed transcripts covering the junction between
306 *cifA* and *cifB*. However, transcripts covering this junction were much more similar to expression
307 levels in *cifA*, while expression of *cifB* was nine-fold less. Therefore, as *cifA* and *cifB* are
308 separated by only 76 bp, distinguishing between 3' UTRs from *cifA* and full *cifA-cifB* transcripts
309 is not possible.
310
311 We next used two computational methods to test for a potential operon between *cifA* and *cifB*
312 using our RNAseq analyses. After mapping reads to the *w*Mel assembly, we used the resulting
313 BAM files as input to Rockhopper (McClure, et al. 2013). The program was able to correctly
314 identify known operons in *w*Mel (such as the T4SS WD0004-WD0008 and the ribosomal protein
315 operon) but it did not identify *cifA* and *cifB* as an operon. We also used a sliding-window
316 approach, using pileup files generated as part of the mapping, to identify correlations between
317 genomic position and gene expression drops in the RNAseq data, as in (Fortino, et al. 2014).The
318 two open reading frames for *cifA* and *cifB* span positions 617223-618647 and 618723-622223,
319 respectively. From positions 618600 to 618700, we observe a significant positive correlation
320 between coverage and genomic location (Pearson Correlation = 0.99, $p < 0.001$). However,

bioRxiv preprint doi: https://doi.org/10.1101/180075; this version posted August 24, 2017. The copyright holder for this preprint (which was not certified by peer review) is the author/funder. All rights reserved. No reuse allowed without permission.

321 across the junction between *cifA* and *cifB* (position 618700), we saw a very large drop in gene
322 expression in both males and females (from an average coverage of 4616 to 38 per position).
323 This result suggests that *cifA* and *cifB* are not co-transcribed.
324
325 Finally, we clustered the *w*Mel *cif* genes based on their similarity in expression across
326 *Drosophila* development (Supplemental Figure S1). *cifA* did not group with *cifB* in *w*Mel (Figure
327 3), suggesting that these two genes are not co-regulated. Indeed, the pattern of *cifA* expression
328 differs strikingly from that of *cifB*. *cifB* is expressed during embryogenesis and generally down-
329 regulated in pupae and adults, while *cifA* is highly expressed in adult males and females and late
330 time points during embryogenesis (Figure 1). Curiously, the expression profile of *cifA* in flies
331 during development is most closely correlated with the *wsp* locus WD1063 (Figure 3).
332
333 **New Protein Domain Predictions are Variable Across the Cif Phylogeny**
334 We recovered the four previously identified phylogenetic types (LePage, et al. 2017). Here, our
335 analyses include additional strains that cause reproductive parasitism beyond CI
336 (parthenogenesis and male-killing, Table 1), and the more divergent Type IV paralogs for *cifA*,
337 so far identified in B-Supergroup *Wolbachia*. We recover a set of Type III alleles from *w*Uni, a
338 strain that induces parthenogenesis in the parasitoid wasp, *Muscidifurax uniraptor* (Stouthamer,
339 et al. 1993). The *w*Bol1-b strain, a male-killer that has retained CI capabilities (Hornett, et al.
340 2008), has alleles belonging to both Type I and Type IV.
341
342 Homologs and predicted protein domains of CifA and CifB for all four phylogenetic types
343 (LePage, et al. 2017) from *Wolbachia* strains that cause CI, parthenogenesis, male-killing, or no

bioRxiv preprint doi: https://doi.org/10.1101/180075; this version posted August 24, 2017. The copyright holder for this preprint (which was not certified by peer review) is the author/funder. All rights reserved. No reuse allowed without permission.

reproductive phenotype were characterized by HHpred homology and domain structure prediction software (Söding, et al. 2005). Search parameters are described in the methods. Several new prominent protein domains (as determined by the presence of multiple highly significant structural predictions within a region), herein referred to as "modules", were identified for each CifA and CifB protein sequence. In Table 2 we list the prominent module annotations identified across CifA and CifB Types. Multiple structural hits within a region can be explained by the homology of the significant domains predictions to each other.

For CifA, three main modules were annotated (Figure 4A, Table 2). First, the most N-terminal module (ModA-1) in Type I, II and III variants shows homology to Catalase-rel ($p = 0.001$-0.003), which is predicted to catalyze the breakdown of hydrogen peroxide (Chelikani, et al. 2004) (Type I) and protect the cell from toxic effects, or VirJ ($p = 0.002$-0.003), a bacterial virulence protein and component of T4SS secretion systems (Pantoja, et al. 2002) (Types II and III). The second CifA module in the central region (ModA-2) has homology to a caspase recruitment domain ($p = 0.005$-0.009), venom and toxin-related domains ($p \leq 0.001$), and a thermal regulator protein ($p = 0.002$). The very significant homology to a toxin is interesting, given that CifA was hypothesized to act as an antitoxin. Notably, CifA is required for and enhances the induction of CI (LePage, et al. 2017), which contradicts its proposed function as simply an antitoxin (Beckmann, et al. 2017). The last CifA module in the C-terminal region (ModA-3) has multiple strong hits to a STE-like transcription factor ($p \leq 0.001$). There were additional annotations that emerged due to weak or singular matches. In Type IV variants, there is a separate N-terminal region that shares homology with a conserved eukaryotic family with potential methyltransferase activity, FAM86 ($p = 0.003$). Most Type I alleles have C-terminal

bioRxiv preprint doi: https://doi.org/10.1101/180075; this version posted August 24, 2017. The copyright holder for this preprint (which was not certified by peer review) is the author/funder. All rights reserved. No reuse allowed without permission.

homology to a nuclear cap-binding protein that binds RNA (p = 0.010 – 0.020). WOHa1, WOBol1b, and WOSol have an additional N-terminal region containing a conserved domain of unknown function (p = <0.001 – 0.005). Type IV genes have a yeast-like salt tolerance down-regulator domain NST1 (p = 0.003). Lastly, WOVit4 and *w*Uni lack the most N-terminal CifA homology region, ModA-1.

For CifB, three main modules were defined (Figure 4B, Table 2). The first (ModB-1) and second (ModB-2) most N-terminal regions both have matches to the PDDEXK nuclease family (p < 0.001), the HSDR_N restriction enzyme (p = <0.001-0.010), and domains of unknown function (DUF1052, DUF91). The third module, found only in the Type I C-terminus (ModB-3), has very strong homology to a number of ubiquitin-modification and peptidase domains (p < 0.001), as well as YopJ, which in *Yersinia*, aids in infecting a eukaryotic host (Paquette, et al. 2012) (p = <0.001-0.020). ModB-3 contains the catalytic residue associated with toxicity/CI function in CidB (Beckmann, et al. 2017). In addition to the annotated modules, all Type I alleles except WOBol1b and WORiB have a single hit to a conserved domain of unknown function in the N-terminus (p = 0.001 – 0.005), and Type III alleles (except for *w*AlbB) have a region of homology to a methyltransferase domain (MTS) (p < 0.001). Both Type II and III alleles have a single short hit in the N-terminus to a SecA regulator. WOVitA4 (Type 1) has an extended C-terminus not present in any other alleles, and within that extended C-terminus is an additional peptidase/YopT-like region, similar to ModB-3. CifB Type IV alleles (WOAlbB, WOPip2, and *w*Bol1-b) were not included in the phylogenetic reconstruction, as they are highly divergent and not reciprocal blasts of WOMelB *cifB*. Despite their divergence, these Type IV CifB alleles have similar structures to Type II and III alleles: two PDDEXK-like modules, and no Ulp-1-like

bioRxiv preprint doi: https://doi.org/10.1101/180075; this version posted August 24, 2017. The copyright holder for this preprint (which was not certified by peer review) is the author/funder. All rights reserved. No reuse allowed without permission.

module three (Supplemental Figure S3). Full structural schematics with exact coordinates and homology regions for each allele are available in the supplemental material (Supplemental Figures S2 and S3), as are all significant domain hits with associated p-values and extended descriptions (Supplemental Tables S1 and S2).

CifA and CifB Codiverge

Initial phylogenetic trees based on core amino acid sequences of Type I-III variants of CifA and CifB exhibited similar trees (LePage, et al. 2017). Here we statistically ground the inference of codivergence using the largest set of *Wolbachia* homologs to date. We quantified congruence between the CifA and CifB phylogenetic trees for Types I-III (Supplemental File S1) using Matching Cluster (MC) and Robinson–Foulds (RF) tree metrics (Bogdanowicz and Giaro 2013; Bogdanowicz, et al. 2012; Robinson and Foulds 1981), with normalized distances ranging from 0.0 (complete congruence) to 1.0 (complete incongruence). Results show strong levels of congruence between CifA and CifB ($p < 0.00001$ for both, normalized MC = 0.06 and normalized RF = 0.125). To further statistically validate the inference of codivergence, we measured the correlation between patristic distance matrices for CifA and CifB using the Mantel test (Mantel 1967). Results demonstrate a high degree of correlation between patristic distance matrices, and through permutation show that independent evolution of CifA and CifB is highly unlikely (Pearson correlation coefficient = 0.905, $p = 0.00001$).

Cif Proteins Evolve Rapidly

Amino acid sequence conservation across the full length of the Cif proteins was determined and compared to *Wolbachia* amino acid sequences of genes that either have signatures of

bioRxiv preprint doi: https://doi.org/10.1101/180075; this version posted August 24, 2017. The copyright holder for this preprint (which was not certified by peer review) is the author/funder. All rights reserved. No reuse allowed without permission.

413 recombination and directional section (Wsp, *Wolbachia* surface protein) or have not undergone
414 extensive recombination and directional selection (FtsZ, cell division protein). Wsp protein
415 sequences exhibit considerable divergence (mean conservation = 0.85), with very few sites in a
416 row being completely conserved (Figure 5A). In contrast, FtsZ is relatively conserved (mean
417 conservation = 0.94), and most of the divergence is clustered at the C-terminus (Figure 5B).
418 Mean conservation for the Cif protein sequences were lower than Wsp - 0.83 for Type I CifA
419 alleles (Figure 5C) and 0.82 for Type I CifB alleles (Figure 5E, Table 3). When all Cif alleles
420 were considered, mean conservation was even further reduced - 0.58 for CifA (Figure 5D) and
421 0.43 for CifB (Figure 5F). The lower average conservation of CifB genes is in part due to the
422 many insertions and deletions in the alignment, and the missing C-terminal deubiquitylase
423 region, ModB-3, of the Type II and III alleles. Thus, several CifB proteins apparently lack this
424 activity, and whether these variants cause CI remains to be determined. Importantly, although the
425 CifB proteins are highly divergent, the catalytic residue (red dot in Figures 5E and 5F) in the
426 deubiquitylating module of CifB is unique to and completely conserved for the Type I alleles.
427 The Cif proteins have extensive amounts of diversity, with completely conserved amino acids
428 distributed across the length of the protein, and not confined to any particular regions (Figure
429 5C-F, Supplemental Tables S3-S6). There were significant differences in the level of
430 conservation between modules and non-module regions for the Type I alignments of both CifA
431 ($F_{3,495} = 11.75$, $p = 0.0021$) and CifB ($F_{3,1195} = 11.75$, $p = 1.38e-07$) (Table 3). The only module
432 that had significantly higher conservation than the non-module regions of the alignment was
433 ModB-1 ($p = 0.0173$). The *w*Mel strain contains the (P)D-(D/E)XK motif (blue dots in Figures
434 5E and 5F) (Kosinski, et al. 2005), but it is less than 80% conserved across strains despite the
435 higher average conservation of this module. In contrast, ModA-3 and ModB-3 are significantly

bioRxiv preprint doi: https://doi.org/10.1101/180075; this version posted August 24, 2017. The copyright holder for this preprint (which was not certified by peer review) is the author/funder. All rights reserved. No reuse allowed without permission.

436 less conserved than the non-module regions of the corresponding proteins (CifA, p = 0.0400;
437 CifB, p = 0.0001).
438
439 **Cif Module Presence Generally Predicts Reproductive Phenotype**
440 We used the *w*Mel predicted Cif modules as a seed to search for the presence of homologous
441 modules across *Wolbachia* genome sequences using tblastn (Figure 6). In strains with more
442 divergent Cif Types, we report modules that were expected based on the HHpred results, but not
443 recovered with tblastn due to sequence divergence from WOMelB. For example, the WOSuziC
444 and WORiC ModA-1 (Catalase-rel in *w*Mel and other Type I, VirJ in Type II and III) was not
445 recovered. Additionally, we recover homologous modules outside of the annotated *cif* open
446 reading frames, such as the chromosomal region with a ModB-3 (Ulp-1-like) region in *w*No. The
447 high number of modules in *w*Suzi and *w*Ri are due to the presence of a duplicated set of Type I
448 *cifs*. All arthropod-infecting strains, with the exception of *w*Au (a non-CI inducing strain),
449 contained at least one recovered module. This includes the bed-bug mutualist *w*Cle, found in
450 Supergroup-F, and two strains that have lost CI abilities, *w*Uni and *w*Tpre. Importantly, all
451 strains that are known to be capable of inducing or rescuing CI have four or more recovered
452 modules, though they do not necessarily have ModB-3, which contains the catalytic residue
453 implicated in CI function (Beckmann, et al. 2017). The non-CI strains have fewer recovered
454 modules: ModB-1 in *w*Tpre, ModB-1 and -2 in *w*Uni, ModA-3 in *w*Cle. and no modules in *w*Au
455 and the nematode-infecting strains. *w*Uni is a unique case, where we identified *cif* alleles in the
456 genome, but recovered relatively few modules. The CifA modules are either missing (Figure 4A)
457 or divergent enough from WOMelB that they were not considered a positive match. The two N-
458 terminal *w*Uni CifB modules, ModB-1 and ModB-2, are relatively more conserved, and the

bioRxiv preprint doi: https://doi.org/10.1101/180075; this version posted August 24, 2017. The copyright holder for this preprint (which was not certified by peer review) is the author/funder. All rights reserved. No reuse allowed without permission.

459 ModB-3 is missing due to the truncated C-terminus present in all non-Type I CifB alleles (Figure
460 4B). wAlbB and *w*No, both CI-inducing strains with Type III and IV alleles, have fewer
461 recovered modules, but this is congruent with the more divergent nature of those Cif types. We
462 recovered many modules in *w*Suzi, which is a strain not known to induce CI (Cattel, et al. 2016;
463 Hamm, et al. 2014). This discrepancy between *cif* presence and absence of a reproductive
464 phenotype might be explained by the disrupted Type II *cifA* in *w*Suzi. The split WOSuziC
465 sequenced was concatenated to allow for a more robust phylogenetic reconstruction (Figure 4),
466 but it is in fact disrupted by a transposase (Conner, et al. 2017). However, having a functional set
467 of Type I *cif* alleles appears to be sufficient for CI-induction in other strains (Beckmann, et al.
468 2017; LePage, et al. 2017), so it is not clear how inactivation of the Type II alleles here may
469 affect the final CI phenotype. Strain *w*Di, infecting the Asian citrus psyllid *Diaphorina citri*, has
470 no identified reproductive phenotype, but only contains a single module: ModB-1.
471
472 The lack of evidence for homologous *cif* genes in the nematode-infecting *Wolbachia* agrees with
473 previous findings (LePage, et al. 2017) that CI-function is restricted to the A+B-Supergroup
474 clade (likely due to WO phage activity), and the absence of WO phages for the nematode-
475 infecting strains (Gavotte, et al. 2007). The loss of CI within the A and B Supergroups is likely a
476 derived trait due to the rapid evolution of prophage WO (Ishmael, et al. 2009; Kent, et al.
477 2011b), and relaxed selection after transition to a new reproductive phenotype. The low number
478 of modules identified in such strains is consistent with gene degradation and loss.
479
480 To further explore the conservation of the *cif* genes across the sequenced *Wolbachia*, and to
481 uncover diversity that may be present in other genomes, we searched the WGS databases for

bioRxiv preprint doi: https://doi.org/10.1101/180075; this version posted August 24, 2017. The copyright holder for this preprint (which was not certified by peer review) is the author/funder. All rights reserved. No reuse allowed without permission.

recently sequenced genomic scaffolds from *Wolbachia* infecting the *Nomada* bees (*w*Nleu, *w*Nla, *w*Npa, *w*Nfe) (Gerth and Bleidorn 2016), *Drosophila inocompta* (*w*Inc_Cu)(Wallau, et al. 2016), and *Laodelphax striatellus* (*w*Stri) (GenBank Accession Number NZ_LRUH00000000.1) using HMMER. Only for *w*Stri do we have direct evidence of CI induction (Noda, et al. 2001) yet the *w*Stri and *w*Inc_Cu WGS projects each contain only one *cif* locus, with distant homology to *cifA* (~25% identify across 60% of the *w*Mel protein). Based on HHpred analyses, the *w*Stri homolog (WP_063631193.1) contains none of the domain modules associated with *cifA.* The *w*Inc_Cu homolog (WP_070356873.1) contains three modules: an N-terminal Catalase-rel domain and an internal Ectatomin domain, followed by the STE like transcriptional factor domain. Because these are incomplete genome projects, it is possible that other *cif* homologs have been missed due to the current sequencing coverage. Alternatively, it is possible that other, as yet undiscovered, mechanisms of reproductive manipulation exist in these strains. In contrast, the *Nomada*-associated *Wolbachia* contain a large repertoire of *cif* homologs, including Type I, II, III, IV and several homologs with variations on the Type IV domain architecture for *cifA* (Supplemental Figure S4). The *Nomada Wolbachia* all harbor Type II *cifB* homologs and each of the strains harbors either duplicates of this *cifB* type or novel domain architectures for *cifB* including an N-terminal Oleosin domain and a C-terminal Ulp-1 domain (Supplemental Figure S4).

Discussion

We explored three key features of *cif* evolution: (i) the toxin-antitoxin operon hypothesis, (ii) potential enzymatic and regulatory functions across the *cifA* and *cifB* phylogenies, and (iii) the conservation and diversity of *cif* genes across strains with different host-manipulation

bioRxiv preprint doi: https://doi.org/10.1101/180075; this version posted August 24, 2017. The copyright holder for this preprint (which was not certified by peer review) is the author/funder. All rights reserved. No reuse allowed without permission.

505 phenotypes. We provide multiple lines of evidence that *cifA* and *cifB* do not comprise an operon
506 in *w*Mel, including quantifications of transcription and *in silico* operon predictors. Moreover,
507 expression of *cifA* and *cifB* across host development are not correlated with each other. In fact,
508 *cifB* expression does not significantly correlate with any other *Wolbachia* locus. Combined with
509 the drastic drop off in expression across the short junction between *cifA* and *cifB*, and negative
510 results from the operon prediction software, we conclude that *cifA* and *cifB* are not co-transcribed
511 or co-regulated as an operon in *w*Mel, the *Wolbachia* strain currently used in mosquito control
512 programs. While we think it unlikely that the *cif* genes are regulated and transcribed in
513 drastically different ways across closely related *cif* Types, more detailed analyses from a variety
514 of strains would be beneficial for developing a comprehensive understanding of the factors
515 regulating expression of these genes. It is especially interesting that synteny has generally been
516 maintained across prophage WO regions, despite the high level of recombination and
517 rearrangements in prophage WO and *Wolbachia* genomes (Baldo, et al. 2006a; Ellegaard, et al.
518 2013; Kent, et al. 2011a). It is not clear if there is an advantage (and what the advantage may be)
519 to maintaining syntenic orientation of these two genes; perhaps this feature can be attributed to
520 their location within prophage WO and/or functions associated with the ability of *cifA* and *cifB* to
521 act synergistically to induce CI (LePage, et al. 2017). Since type IV secretion system genes and
522 their predicted effectors are scattered across the *Wolbachia* genome (Rice, et al. 2017; Wu, et al.
523 2004) gene products involved in *Wolbachia*-host interactions can function together even when
524 the genes encoding them are not syntenic. We conclude that *cifA* and *cifB* do not comprise an
525 operon, and do not act strictly as a toxin-antitoxin system due to the requirement of both proteins
526 for the induction of CI in the insect host. Determining how *cifA* and *cifB* expression is regulated
527 in the insect host will greatly benefit vector control programs that use *Wolbachia*-mediated CI.

bioRxiv preprint doi: https://doi.org/10.1101/180075; this version posted August 24, 2017. The copyright holder for this preprint (which was not certified by peer review) is the author/funder. All rights reserved. No reuse allowed without permission.

528

529 Despite the conservation of gene order, Cif proteins showed extensive amounts of divergence
530 and differences in domain structure as previously reported (LePage, et al. 2017). Here, the levels
531 of amino acid conservation in the Cifs are lower than FtsZ and Wsp, the latter of which is known
532 to recombine and be subject to directional selection. The conservation of the catalytic residue in
533 the C-terminal deubiquitylase domain is an important feature of CidB (Beckmann, et al. 2017).
534 However, only Type I of the four identified Types has this domain. Additionally, strains known
535 to induce CI, such as *w*AlbB and *w*No have no Type I alleles, implying that the Ulp-1 region
536 may not be essential for inducing CI. The complete, functional capacity of Types I-IV has yet to
537 be explored *in vivo*, but is a promising direction for understanding the evolution of *Wolbachia*-
538 host associations.

539

540 Based on what is known about *Wolbachia* biology, some of the protein domains may be
541 especially good candidates for further study and *in vivo* functional characterization. Predicted
542 PDDEXK-like domains are present in all four CifB types. Given the predicted interaction of
543 these domains with DNA (Kosinski, et al. 2005), and the presence of these domains across CifB
544 proteins, determining if and how these regions interact with host (*Wolbachia* or insect) DNA,
545 and whether or not they contribute to CI function would be useful in understanding the consistent
546 presence of this module. Another good candidate for further exploration is the predicted
547 methyltransferase domain in several Type III CifB proteins, as *Wolbachia* infection has been
548 linked to changes in host genome methylation in several insects (LePage, et al. 2014; Negri, et al.
549 2009; Ye, et al. 2013), though knockout of *Drosophila* methyltransferases does not alter CI
550 levels (LePage, et al. 2014). Likewise, the antioxidant catalase domain is noteworthy as these

bioRxiv preprint doi: https://doi.org/10.1101/180075; this version posted August 24, 2017. The copyright holder for this preprint (which was not certified by peer review) is the author/funder. All rights reserved. No reuse allowed without permission.

551 domains decompose hydrogen peroxide into water and oxygen and thus protect cells from its
552 toxic effects, which are present in *Wolbachia*-infected spermatocytes (Brennan, et al. 2012).
553
554 *Wolbachia* strains that have lost CI have a strong signature of *cif* gene degradation and loss. The
555 two parthenogenesis-inducing strains (*w*Tpre and *w*Uni) appear to be at different places in this
556 process of gene loss, with divergent Cif amino acid sequences recovered for *w*Uni, but only one
557 PDDEXK module identified in *w*Tpre. There are several explanations for this. *w*Uni is likely a
558 more recent transition to parthenogenesis, as it is closely related to a CI strain (*w*VitA) (Baldo, et
559 al. 2006b; Newton, et al. 2016). In comparison, *w*Tpre is part of a unique clade of *Wolbachia* that
560 all induce parthenogenesis in *Trichogramma* wasps (Rousset, et al. 1992; Schilthuizen and
561 Stouthamer 1997; Werren, et al. 1995). This strain has lost its WO phage association and only
562 has relics of WO phage genes (Gavotte, et al. 2007; Lindsey, et al. 2016). Additionally, the two
563 strains that independently transitioned to the parthenogenesis phenotype have evolved separate
564 mechanisms for doing so (Gottlieb, et al. 2002; Stouthamer and Kazmer 1994). Differences in
565 time since transition to the parthenogenesis phenotype, phage WO associations, and mechanisms
566 of parthenogenesis induction likely all play a role in the rate of *cif* gene degradation.
567
568 Based on our analyses, we propose three avenues of research on the function of the Cif proteins.
569 First, functional confirmation of the newly annotated modules will be important to understanding
570 how these genes function enzymatically. In total, we predict six modules in the Cif protein
571 sequence homologs, with varying degrees of confidence (Supplemental Tables S1 and S2
572 Tables). For some of these modules, straightforward experiments can be designed in model
573 systems (such as *Saccharomyces*) to determine if their predicted function is correct, as has been

bioRxiv preprint doi: https://doi.org/10.1101/180075; this version posted August 24, 2017. The copyright holder for this preprint (which was not certified by peer review) is the author/funder. All rights reserved. No reuse allowed without permission.

574 done for CidB (Beckmann, et al. 2017) and countless other bacterial effectors (Archuleta, et al.
575 2011; Kramer, et al. 2007; Siggers and Lesser 2008). Second, necessity and importance of these
576 modules to the CI phenotype can be assessed in the *Drosophila* model, where the induction of
577 the phenotype and rescue is straightforward (LePage, et al. 2017). Finally, we suggest that
578 although the discovery of these genes is fundamental, it is clear from this analysis that we have
579 not comprehensively evaluated or identified the mechanisms behind CI and other reproductive
580 manipulations. The gene characterization analyses described here reveal new and relevant
581 annotations, substantial unknown sequence regions across all of the phylogenetic types, missing
582 deubiquitylase domains in particular CI strains, and a coevolving, phylogenetic relationship
583 across the Cif trees. Importantly, the locus and mechanism behind rescuing CI are still unknown,
584 as is the exact mechanism by which all Cif proteins induce CI. Therefore, the recent discovery of
585 these genes, and the gene characterization analyses described here, pave the most comprehensive
586 road to date for investigating key mechanisms of the *Wolbachia*-host symbiosis.
587

588 **Acknowledgments**

589 This work was supported by the National Science Foundation (DEB 1501227 to A.R.I.L., IOS
590 1456545 to I.L.G.N., and IOS 1456778 to S.R.B); the United States Department of Agriculture
591 (NIFA 2016-67011-24778 to A.R.I.L.); the National Institutes of Health (R21 HD086833 and
592 R01 AI132581 to S.R.B.); and Robert and Peggy van den Bosch Memorial Scholarships to
593 A.R.I.L. We thank J. Dylan Shropshire for feedback on an earlier draft of the manuscript.

bioRxiv preprint doi: https://doi.org/10.1101/180075; this version posted August 24, 2017. The copyright holder for this preprint (which was not certified by peer review) is the author/funder. All rights reserved. No reuse allowed without permission.

References

Abascal F, Zardoya R, Posada D 2005. ProtTest: selection of best-fit models of protein evolution. Bioinformatics 21: 2104-2105.

Archuleta TL, et al. 2011. The *Chlamydia* effector chlamydial outer protein N (CopN) sequesters tubulin and prevents microtubule assembly. J Biol Chem 286: 33992-33998.

Baldo L, Bordenstein S, Wernegreen JJ, Werren JH 2006a. Widespread recombination throughout *Wolbachia* genomes. Mol Biol Evol 23: 437-449.

Baldo L, et al. 2006b. Multilocus sequence typing system for the endosymbiont *Wolbachia pipientis*. Appl Environ Microbiol 72: 7098-7110. doi: 10.1128/aem.00731-06

Baldo L, Lo N, Werren JH 2005. Mosaic nature of the *Wolbachia* surface protein. J Bacteriol 187: 5406-5418.

Bandi C, Anderson TJC, Genchi C, Blaxter ML 1998. Phylogeny of *Wolbachia* in filarial nematodes. Proc R Soc Lond B 265: 2407-2413.

Beckmann JF, Fallon AM 2013. Detection of the *Wolbachia* protein WPIP0282 in mosquito spermathecae: implications for cytoplasmic incompatibility. Insect Biochem Mol Biol 43: 867-878. doi: 10.1016/j.ibmb.2013.07.002

Beckmann JF, Ronau JA, Hochstrasser M 2017. A *Wolbachia* deubiquitylating enzyme induces cytoplasmic incompatibility. Nat Micro 2: 17007. doi: 10.1038/nmicrobiol.2017.7

Bian GW, Xu Y, Lu P, Xie Y, Xi ZY 2010. The endosymbiotic bacterium *Wolbachia* induces resistance to dengue virus in *Aedes aegypti*. PLoS Path 6. doi: 10.1371/journal.ppat.1000833

bioRxiv preprint doi: https://doi.org/10.1101/180075; this version posted August 24, 2017. The copyright holder for this preprint (which was not certified by peer review) is the author/funder. All rights reserved. No reuse allowed without permission.

614 Bogdanowicz D, Giaro K 2013. On a matching distance between rooted phylogenetic trees. Intl J
615 Appl Math Comp Sci 23: 669-684.

616 Bogdanowicz D, Giaro K, Wróbel B 2012. TreeCmp: Comparison of trees in polynomial time.
617 Evol Bioinf Online 8: 475.

618 Bordenstein SR, Bordenstein SR 2016. Eukaryotic association module in phage WO genomes
619 from *Wolbachia*. Nat Commun 7.

620 Bordenstein SR, Marshall ML, Fry AJ, Kim U, Wernegreen JJ 2006. The tripartite associations
621 between bacteriophage, *Wolbachia*, and arthropods. PLoS Path 2: e43. doi:
622 10.1371/journal.ppat.0020043

623 Bordenstein SR, O'hara FP, Werren JH 2001. *Wolbachia*-induced incompatibility precedes other
624 hybrid incompatibilities in *Nasonia*. Nature 409: 707-710.

625 Bourtzis K, et al. 2014. Harnessing mosquito–*Wolbachia* symbiosis for vector and disease
626 control. Acta Trop 132, Supplement: S150-S163. doi: 10.1016/j.actatropica.2013.11.004

627 Brennan L, Haukedal J, Earle J, Keddie B, Harris H 2012. Disruption of redox homeostasis leads
628 to oxidative DNA damage in spermatocytes of *Wolbachia*‐infected *Drosophila simulans*. Insect
629 Mol Biol 21: 510-520.

630 Brooks AW, Kohl KD, Brucker RM, van Opstal EJ, Bordenstein SR 2016. Phylosymbiosis:
631 Relationships and functional effects of microbial communities across host evolutionary history.
632 PLoS Biol 14: e2000225.

bioRxiv preprint doi: https://doi.org/10.1101/180075; this version posted August 24, 2017. The copyright holder for this preprint (which was not certified by peer review) is the author/funder. All rights reserved. No reuse allowed without permission.

633 Brucker RM, Bordenstein SR 2013. The hologenomic basis of speciation: gut bacteria cause
634 hybrid lethality in the genus *Nasonia*. Science 341: 667-669.

635 Caporaso JG, et al. 2010. QIIME allows analysis of high-throughput community sequencing
636 data. Nat Methods 7: 335.

637 Capra JA, Singh M 2007. Predicting functionally important residues from sequence
638 conservation. Bioinformatics 23: 1875-1882.

639 Cattel J, et al. 2016. *Wolbachia* in European populations of the invasive pest *Drosophila suzukii*:
640 regional variation in infection frequencies. PLoS One 11: e0147766.

641 Chelikani P, Fita I, Loewen PC 2004. Diversity of structures and properties among catalases.
642 Cell Mol Life Sci 61: 192-208.

643 Conner WR, et al. 2017. Genome comparisons indicate recent transfer of wRi-like *Wolbachia*
644 between sister species *Drosophila suzukii* And *D. subpulchrella*. bioRxiv: 135475.

645 Dedeine F, et al. 2001. Removing symbiotic *Wolbachia* bacteria specifically inhibits oogenesis
646 in a parasitic wasp. Proc Natl Acad Sci 98: 6247-6252. doi: 10.1073/pnas.101304298

647 Duron O, Fort P, Weill M 2006. Hypervariable prophage WO sequences describe an unexpected
648 high number of *Wolbachia* variants in the mosquito *Culex pipiens*. Proc R Soc Lond B 273: 495-
649 502.

650 Eddy SR 2011. Accelerated profile HMM searches. PLoS Comput Biol 7: e1002195.

651 Edgar RC 2004. MUSCLE: multiple sequence alignment with high accuracy and high
652 throughput. Nucleic Acids Res 32: 1792-1797.

bioRxiv preprint doi: https://doi.org/10.1101/180075; this version posted August 24, 2017. The copyright holder for this preprint (which was not certified by peer review) is the author/funder. All rights reserved. No reuse allowed without permission.

653 Ellegaard KM, Klasson L, Naslund K, Bourtzis K, Andersson SGE 2013. Comparative genomics
654 of *Wolbachia* and the bacterial species concept. PLoS Genet 9: e1003381. doi:
655 10.1371/journal.pgen.1003381

656 Felsenstein J 1989. PHYLIP-phylogeny inference package (version 3.2). Cladistics 5: 6.

657 Fortino V, Smolander O-P, Auvinen P, Tagliaferri R, Greco D 2014. Transcriptome dynamics-
658 based operon prediction in prokaryotes. BMC Bioinformatics 15: 145.

659 Gavotte L, et al. 2007. A survey of the bacteriophage WO in the endosymbiotic bacteria
660 *Wolbachia*. Mol Biol Evol 24: 427-435. doi: 10.1093/molbev/msl171

661 Gerth M, Bleidorn C 2016. Comparative genomics provides a timeframe for *Wolbachia*
662 evolution and exposes a recent biotin synthesis operon transfer. Nat Micro 2: 16241.

663 Gottlieb Y, Zchori-Fein E, Werren JH, Karr TL 2002. Diploidy restoration in *Wolbachia*-
664 infected *Muscidifurax uniraptor* (Hymenoptera: Pteromalidae). J Invertebr Pathol 81: 166-174.

665 Gutzwiller F, et al. 2015. Dynamics of *Wolbachia pipientis* gene expression across the
666 *Drosophila melanogaster* life cycle. G3: Genes| Genomes| Genetics 5: 2843-2856.

667 Hamm CA, et al. 2014. *Wolbachia* do not live by reproductive manipulation alone: infection
668 polymorphism in *Drosophila suzukii* and *D. subpulchrella*. Mol Ecol 23: 4871-4885.

669 Hilgenboecker K, Hammerstein P, Schlattmann P, Telschow A, Werren JH 2008. How many
670 species are infected with *Wolbachia*? - A statistical analysis of current data. FEMS Microbiol
671 Lett 281: 215-220. doi: 10.1111/j.1574-6968.2008.01110.x

bioRxiv preprint doi: https://doi.org/10.1101/180075; this version posted August 24, 2017. The copyright holder for this preprint (which was not certified by peer review) is the author/funder. All rights reserved. No reuse allowed without permission.

672 Hoerauf A, et al. 1999. Tetracycline therapy targets intracellular bacteria in the filarial nematode
673 *Litomosoides sigmodontis* and results in filarial infertility. J Clin Invest 103: 11-18.

674 Hoffmann AA, et al. 2011. Successful establishment of *Wolbachia* in *Aedes* populations to
675 suppress dengue transmission. Nature 476: 454-U107. doi: 10.1038/nature10356

676 Hornett EA, et al. 2008. You can't keep a good parasite down: evolution of a male-killer
677 suppressor uncovers cytoplasmic incompatibility. Evolution 62: 1258-1263. doi: 10.1111/j.1558-
678 5646.2008.00353.x

679 Hosokawa T, Koga R, Kikuchi Y, Meng XY, Fukatsu T 2010. *Wolbachia* as a bacteriocyte-
680 associated nutritional mutualist. Proc Natl Acad Sci 107: 769-774. doi:
681 10.1073/pnas.0911476107

682 http://python.org. Python Language Reference, version 2.7.

683 Hughes GL, Koga R, Xue P, Fukatsu T, Rasgon JL 2011. *Wolbachia* infections are virulent and
684 inhibit the human malaria parasite *Plasmodium falciparum* in *Anopheles Gambiae*. PLoS Path 7:
685 e1002043. doi: 10.1371/journal.ppat.1002043

686 Hurst GD, et al. 1999. Male–killing *Wolbachia* in two species of insect. Proc R Soc Lond B 266:
687 735-740.

688 Hurvich CM, Tsai CL 1993. A corrected Akaike information criterion for vector autoregressive
689 model selection. Journal of Time Series Analysis 14: 271-279.

690 Ishmael N, et al. 2009. Extensive genomic diversity of closely related *Wolbachia* strains.
691 Microbiology 155: 2211-2222. doi: 10.1099/mic.0.027581-0

bioRxiv preprint doi: https://doi.org/10.1101/180075; this version posted August 24, 2017. The copyright holder for this preprint (which was not certified by peer review) is the author/funder. All rights reserved. No reuse allowed without permission.

692 Jaenike J, Dyer KA, Cornish C, Minhas MS 2006. Asymmetrical reinforcement and *Wolbachia*
693 infection in *Drosophila*. PLoS Biol 4: e325.

694 Kambris Z, Cook PE, Phuc HK, Sinkins SP 2009. Immune activation by life-shortening
695 *Wolbachia* and reduced filarial competence in mosquitoes. Science 326: 134-136. doi:
696 10.1126/science.1177531

697 Katoh K, Standley DM 2013. MAFFT multiple sequence alignment software version 7:
698 improvements in performance and usability. Mol Biol Evol 30: 772-780. doi:
699 10.1093/molbev/mst010

700 Kearse M, et al. 2012. Geneious Basic: an integrated and extendable desktop software platform
701 for the organization and analysis of sequence data. Bioinformatics 28: 1647-1649.

702 Kent BN, Funkhouser LJ, Setia S, Bordenstein SR 2011a. Evolutionary genomics of a temperate
703 bacteriophage in an obligate intracellular bacteria (*Wolbachia*). PLoS One 6: e24984.

704 Kent BN, et al. 2011b. Complete bacteriophage transfer in a bacterial endosymbiont (*Wolbachia*)
705 determined by targeted genome capture. Genome Biol Evol 3: 209-218. doi: 10.1093/gbe/evr007

706 Kosinski J, Feder M, Bujnicki JM 2005. The PD-(D/E) XK superfamily revisited: identification
707 of new members among proteins involved in DNA metabolism and functional predictions for
708 domains of (hitherto) unknown function. BMC Bioinformatics 6: 172.

709 Kramer RW, et al. 2007. Yeast functional genomic screens lead to identification of a role for a
710 bacterial effector in innate immunity regulation. PLoS Pathog 3: e21.

bioRxiv preprint doi: https://doi.org/10.1101/180075; this version posted August 24, 2017. The copyright holder for this preprint (which was not certified by peer review) is the author/funder. All rights reserved. No reuse allowed without permission.

711 Landmann F, Orsi GA, Loppin B, Sullivan W 2009. *Wolbachia*-mediated Cytoplasmic
712 Incompatibility is associated with impaired histone deposition in the male pronucleus. PLoS Path
713 5. doi: 10.1371/journal.ppat.1000343

714 Lassy CW, Karr TL 1996. Cytological analysis of fertilization and early embryonic development
715 in incompatible crosses of *Drosophila simulans*. Mechanisms of Development 57: 47-58.

716 LePage DP, Jernigan KK, Bordenstein SR 2014. The relative importance of DNA methylation
717 andDnmt2-mediated epigenetic regulation on *Wolbachia* densities and cytoplasmic
718 incompatibility. PeerJ 2: e678. doi: 10.7717/peerj.678

719 LePage DP, et al. 2017. Prophage WO genes recapitulate and enhance *Wolbachia*-induced
720 cytoplasmic incompatibility. Nature 543: 243-247. doi: 10.1038/nature21391

721 Li B, Dewey CN 2011. RSEM: accurate transcript quantification from RNA-Seq data with or
722 without a reference genome. BMC Bioinformatics 12: 323.

723 Lindsey ARI, Werren JH, Richards S, Stouthamer R 2016. Comparative genomics of a
724 parthenogenesis-inducing *Wolbachia* symbiont. G3: Genes|Genomes|Genetics. doi:
725 10.1534/g3.116.028449

726 Lo N, Casiraghi M, Salati E, Bazzocchi C, Bandi C 2002. How many *Wolbachia* supergroups
727 exist? Mol Biol Evol 19: 341-346.

728 Mantel N 1967. The detection of disease clustering and a generalized regression approach.
729 Cancer Res 27: 209-220.

bioRxiv preprint doi: https://doi.org/10.1101/180075; this version posted August 24, 2017. The copyright holder for this preprint (which was not certified by peer review) is the author/funder. All rights reserved. No reuse allowed without permission.

730 Masui S, Kamoda S, Sasaki T, Ishikawa H 2000. Distribution and evolution of bacteriophage
731 WO in *Wolbachia*, the endosymbiont causing sexual alterations in arthropods. J Mol Evol 51:
732 491-497.

733 McClure R, et al. 2013. Computational analysis of bacterial RNA-Seq data. Nucleic Acids Res
734 41: e140-e140.

735 Miller WJ, Ehrman L, Schneider D 2010. Infectious speciation revisited: impact of symbiont-
736 depletion on female fitness and mating behavior of *Drosophila paulistorum*. PLoS Pathog 6:
737 e1001214.

738 Min K-T, Benzer S 1997. *Wolbachia*, normally a symbiont of *Drosophila*, can be virulent,
739 causing degeneration and early death. Proc Natl Acad Sci 94: 10792-10796. doi:
740 10.1073/pnas.94.20.10792

741 Moreau J, Bertin A, Caubet Y, Rigaud T 2001. Sexual selection in an isopod with *Wolbachia*-
742 induced sex reversal: males prefer real females. J Evol Biol 14: 388-394.

743 Moreira LA, et al. 2009. A *Wolbachia* symbiont in *Aedes aegypti* limits infection with dengue,
744 chikungunya, and *Plasmodium*. Cell 139: 1268-1278. doi: 10.1016/j.cell.2009.11.042

745 Negri H, et al. 2009. Unravelling the *Wolbachia* evolutionary role: the reprogramming of the
746 host genomic imprinting. Proc R Soc Lond B 276: 2485-2491. doi: 10.1098/rspb.2009.0324

747 Newton IL, et al. 2016. Comparative genomics of two closely related *Wolbachia* with different
748 reproductive effects on hosts. Genome Biol Evol 8: 1526-1542. doi: 10.1093/gbe/evw096

bioRxiv preprint doi: https://doi.org/10.1101/180075; this version posted August 24, 2017. The copyright holder for this preprint (which was not certified by peer review) is the author/funder. All rights reserved. No reuse allowed without permission.

749 Noda H, Koizumi Y, Zhang Q, Deng K 2001. Infection density of *Wolbachia* and incompatibility
750 level in two planthopper species, *Laodelphax striatellus* and *Sogatella furcifera*. Insect Biochem
751 Mol Biol 31: 727-737.

752 O'Neill SL, Giordano R, Colbert AME, Karr TL, Robertson HM 1992. 16S ribosomal-RNA
753 phylogenetic analysis of the bacterial endosymbionts associated with cytoplasmic
754 incompatibility in insects. Proc Natl Acad Sci 89: 2699-2702. doi: 10.1073/pnas.89.7.2699

755 Pantoja M, Chen L, Chen Y, Nester EW 2002. *Agrobacterium* type IV secretion is a two‐step
756 process in which export substrates associate with the virulence protein VirJ in the periplasm. Mol
757 Microbiol 45: 1325-1335.

758 Paquette N, et al. 2012. Serine/threonine acetylation of TGFβ-activated kinase (TAK1) by
759 Y*ersinia pestis* YopJ inhibits innate immune signaling. Proc Natl Acad Sci 109: 12710-12715.

760 Pérez F, Granger BE 2007. IPython: a system for interactive scientific computing. Computing in
761 Science & Engineering 9.

762 Randerson JP, Jiggins FM, Hurst LD 2000. Male killing can select for male mate choice: a novel
763 solution to the paradox of the lek. Proc R Soc Lond B 267: 867-874.

764 Rice DW, Sheehan KB, Newton IL 2017. Large-scale identification of *Wolbachia pipientis*
765 effectors. Genome Biol Evol 9: 1925-1937.

766 Robinson DF, Foulds LR 1981. Comparison of phylogenetic trees. Math Biosci 53: 131-147.

767 Ronquist F, et al. 2012. MrBayes 3.2: efficient Bayesian phylogenetic inference and model
768 choice across a large model space. Syst Biol 61: 539-542.

bioRxiv preprint doi: https://doi.org/10.1101/180075; this version posted August 24, 2017. The copyright holder for this preprint (which was not certified by peer review) is the author/funder. All rights reserved. No reuse allowed without permission.

769 Ros VID, Fleming VM, Feil EJ, Breeuwer JAJ 2009. How diverse is the genus *Wolbachia*?
770 Multiple-gene sequencing reveals a putatively new *Wolbachia* supergroup recovered from spider
771 mites (Acari: Tetranychidae). Appl Environ Microbiol 75: 1036-1043. doi: 10.1128/aem.01109-
772 08

773 Rousset F, Bouchon D, Pintureau B, Juchault P, Solignac M 1992. *Wolbachia* endosymbionts
774 responsible for various alterations of sexuality in arthropods. Proc R Soc Lond B 250: 91-98.

775 Schilthuizen M, Stouthamer R 1997. Horizontal transmission of parthenogenesis-inducing
776 microbes in *Trichogramma* wasps. Proc R Soc Lond B 264: 361-366.

777 scikit-bio.org. scikit-bio: core bioinformatics data structures and algorithms in Python.
778 caporasolab.us: Northern Arizona University.

779 Serbus LR, Casper-Lindley C, Landmann F, Sullivan W 2008. The genetics and cell biology of
780 *Wolbachia*-host interactions. Annu Rev Genet 42: 683-707. doi:
781 10.1146/annurev.genet.41.110306.130354

782 Shropshire JD, Bordenstein SR 2016. Speciation by symbiosis: the microbiome and behavior.
783 MBio 7. doi: 10.1128/mBio.01785-15

784 Siggers KA, Lesser CF 2008. The Yeast *Saccharomyces cerevisiae*: a versatile model system for
785 the identification and characterization of bacterial virulence proteins. Cell host & microbe 4: 8-
786 15.

787 Sinkins SP, et al. 2005. *Wolbachia* variability and host effects on crossing type in *Culex*
788 mosquitoes. Nature 436: 257-260.

bioRxiv preprint doi: https://doi.org/10.1101/180075; this version posted August 24, 2017. The copyright holder for this preprint (which was not certified by peer review) is the author/funder. All rights reserved. No reuse allowed without permission.

789 Söding J, Biegert A, Lupas AN 2005. The HHpred interactive server for protein homology
790 detection and structure prediction. Nucleic Acids Res 33: W244-W248.

791 Stamatakis A 2014. RAxML version 8: A tool for phylogenetic analysis and post-analysis of
792 large phylogenies. Bioinformatics. doi: 10.1093/bioinformatics/btu033

793 Stouthamer R, Breeuwer JAJ, Luck RF, Werren JH 1993. Molecular-identification of
794 microorganisms associated with parthenogenesis. Nature 361: 66-68. doi: 10.1038/361066a0

795 Stouthamer R, Kazmer DJ 1994. Cytogenetics of microbe-associated parthenogenesis and its
796 consequences for gene flow in *Trichogramma* wasps. Heredity 73: 317-327. doi:
797 10.1038/hdy.1994.139

798 Stouthamer R, Luck R 1993. Influence of microbe-associated parthenogenesis on the fecundity
799 of *Trichogramma deion* and *T. pretiosum*. Entomol Exp Appl 67: 183-192. doi: 10.1111/j.1570-
800 7458.1993.tb01667.x

801 Stouthamer R, Luck RF, Hamilton WD 1990. Antibiotics cause parthenogenetic *Trichogramma*
802 (Hymenoptera, Trichogrammatidae) to revert to sex. Proc Natl Acad Sci 87: 2424-2427. doi:
803 10.1073/pnas.87.7.2424

804 Sutton E, Harris S, Parkhill J, Sinkins S 2014. Comparative genome analysis of *Wolbachia* strain
805 *w*Au. BMC Genomics 15: 928.

806 Teixeira L, Ferreira Á, Ashburner M 2008. The bacterial symbiont *Wolbachia* induces resistance
807 to RNA viral infections in *Drosophila melanogaster*. PLoS Biol 6: e1000002.

bioRxiv preprint doi: https://doi.org/10.1101/180075; this version posted August 24, 2017. The copyright holder for this preprint (which was not certified by peer review) is the author/funder. All rights reserved. No reuse allowed without permission.

808 Tram U, Sullivan W 2002. Role of delayed nuclear envelope breakdown and mitosis in
809 *Wolbachia*-induced cytoplasmic incompatibility. Science 296: 1124-1126.

810 Turelli M, Hoffmann AA 1991. Rapid spread of an inherited incompatibility factor in California
811 *Drosophila*. Nature 353: 440-442.

812 Walker T, et al. 2011. The *w*Mel *Wolbachia* strain blocks dengue and invades caged *Aedes*
813 *aegypti* populations. Nature 476: 450-U101. doi: 10.1038/nature10355

814 Wallau GL, da Rosa MT, De Re FC, Loreto EL 2016. *Wolbachia* from *Drosophila incompta*:
815 just a hitchhiker shared by *Drosophila* in the New and Old World? Insect Mol Biol 25: 487-499.
816 doi: 10.1111/imb.12237

817 Werren JH, Baldo L, Clark ME 2008. *Wolbachia*: master manipulators of invertebrate biology.
818 Nat Rev Micro 6: 741-751. doi: 10.1038/nrmicro1969

819 Werren JH, Windsor DM 2000. *Wolbachia* infection frequencies in insects: Evidence of a global
820 equilibrium? Proc R Soc Lond B 267: 1277-1285. doi: 10.1098/rspb.2000.1139

821 Werren JH, Zhang W, Guo LR 1995. Evolution and phylogeny of *Wolbachia* - reproductive
822 parasites of arthropods. Proc R Soc Lond B 261: 55-63. doi: 10.1098/rspb.1995.0117

823 Wu M, et al. 2004. Phylogenomics of the reproductive parasite *Wolbachia* pipientis *w*Mel: A
824 streamlined genome overrun by mobile genetic elements. PLoS Biol 2: 327-341. doi:
825 10.1371/journal.pbio.0020069

bioRxiv preprint doi: https://doi.org/10.1101/180075; this version posted August 24, 2017. The copyright holder for this preprint (which was not certified by peer review) is the author/funder. All rights reserved. No reuse allowed without permission.

826 Ye YXH, et al. 2013. Infection with a virulent strain of *Wolbachia* disrupts genome wide-
827 patterns of cytosine methylation in the mosquito *Aedes aegypti*. PLoS One 8: e66482. doi:
828 10.1371/journal.pone.0066482

829 Yen JH, Barr AR 1971. New hypothesis of the cause of cytoplasmic incompatibility in *Culex*
830 *pipiens.* Nature.

831 Zabalou S, et al. 2004. *Wolbachia*-induced cytoplasmic incompatibility as a means for insect pest
832 population control. Proc Natl Acad Sci 101: 15042-15045. doi: 10.1073/pnas.0403853101

833 Zug R, Hammerstein P 2012. Still a host of hosts for *Wolbachia*: Analysis of recent data suggests
834 that 40% of terrestrial arthropod species are infected. PLoS One 7. doi:
835 10.1371/journal.pone.0038544

836

837

bioRxiv preprint doi: https://doi.org/10.1101/180075; this version posted August 24, 2017. The copyright holder for this preprint (which was not certified by peer review) is the author/funder. All rights reserved. No reuse allowed without permission.

Tables

Table 1. Strains used in comparative analyses of *cifA* and *cifB*.

Supergroup	Strain	Host	Reproductive Phenotypes[a]	Accession Number
A	*w*Mel	*Drosophila melanogaster*	CI	NC_002978.6
	*w*MelPop	*Drosophila melanogaster*	CI	AQQE00000000.1
	*w*Rec	*Drosophila recens*	CI	NZ_JQAM00000000.1
	*w*Au	*Drosophila simulans*	None	LK055284.1
	*w*Ha	*Drosophila simulans*	CI	NC_021089.1
	*w*Ri	*Drosophila simulans*	CI	NC_012416.1
	*w*Suzi	*Drosophila suzukii*	None	NZ_CAOU00000000.2
	*w*Uni	*Muscidifurax uniraptor*	PI	NZ_ACFP00000000.1
	*w*VitA	*Nasonia vitripennis*	CI	NZ_MUJM00000000.1
B	*w*AlbB	*Aedes albopictus*	CI	CAGB00000000.1
	*w*No	*Drosophila simulans*	CI	NC_021084.1
	*w*Di	*Diaphorina citri*	Undetermined	NZ_KB223540.1
	*w*Tpre	*Trichogramma pretiosum*	PI	CM003641.1
	*w*VitB	*Nasonia vitripennis*	CI	AERW00000000.1
	*w*Bol1-b	*Hypolimnas bolina*	CI, MK	NZ_CAOH00000000.1
	*w*PipJHB	*Culex quinquefasciatus*	CI	ABZA00000000.1
	*w*PipPel	*Culex pipiens*	CI	NC_010981.1
C	*w*Oo	*Onchocerca ochengi*	OM	NC_018267.1
	*w*Ov	*Onchocerca volvulus*	OM	NZ_HG810405.1
D	*w*Bm	*Brugia malayi*	OM	NC_006833.1
F	*w*Cle	*Cimex lectularius*	OM	NZ_AP013028.1

[a]Reproductive phenotypes include: CI) cytoplasmic incompatibility, PI) parthenogenesis-inducing, MK) male-killing, OM) obligate mutualism, None) no phenotype discovered after assessment, and Undetermined) phenotype was not assayed.

bioRxiv preprint doi: https://doi.org/10.1101/180075; this version posted August 24, 2017. The copyright holder for this preprint (which was not certified by peer review) is the author/funder. All rights reserved. No reuse allowed without permission.

844 **Table 2. Predicted structural modules of Cif proteins.**

Protein	Module[a]	Size Range (AA)	Homology
CifA	ModA-1 ●	24-55	• Catalase-rel, decomposes hydrogen peroxide into water and oxygen • VirJ, bacterial virulence protein and component of T4SS secretion systems
	ModA-2 ●	99-152	• DUF3243, DUF603, domains of unknown function • CARD_MDA5_r1, Caspase activation and recruitment domain • Ectatomin, toxic component of ant venom • Ldr, type I toxin-antitoxin system • lstR, lineage-specific thermal regulator protein
	ModA-3 ●	47-68	• STE, STE-like transcription factor
CifB	ModB-1 ●	97-127	• PDDEXK, PD-(D/E)XK nuclease superfamily • DUF91, Domain of Unknown Function • HSDR_N, type I restriction enzyme R protein N terminus
	ModB-2 ●	122-155	• PDDEXK, PD-(D/E)XK nuclease superfamily • DUF1052, domain of unknown function • HSDR_N, type I restriction enzyme R protein N terminus • RE_XamI, XamI restriction endonuclease
	ModB-3[b] ○	277	• Ulp-1, ubiquitin-like proteases • SUMO, small ubiquitin-related modifier • YopJ, Serine/Threonine acetyltransferase (*Yersinia*) • SseI, deubiquitylase • SidE, Dot/Icm substrate protein

845 [a]Colors next to modules are used throughout the text

846 [b]Only present in Type I

847

848

bioRxiv preprint doi: https://doi.org/10.1101/180075; this version posted August 24, 2017. The copyright holder for this preprint (which was not certified by peer review) is the author/funder. All rights reserved. No reuse allowed without permission.

Table 3. Average amino acid conservation of Cifs and modules.

Protein	Region[a]	Type I	All
CifA	ModA-1	0.94	0.70
	ModA-2	0.82	0.55
	ModA-3	0.77	0.53
	CifA	0.83	0.58
CifB	ModB-1	0.89	0.71
	ModB-2	0.85	0.62
	ModB-3[b]	0.77	0.39
	CifB	0.82	0.43

[a]Module number defined in Table 2

[b]Only present in Type I

bioRxiv preprint doi: https://doi.org/10.1101/180075; this version posted August 24, 2017. The copyright holder for this preprint (which was not certified by peer review) is the author/funder. All rights reserved. No reuse allowed without permission.

853 **Figures**

854 **Figure 1**

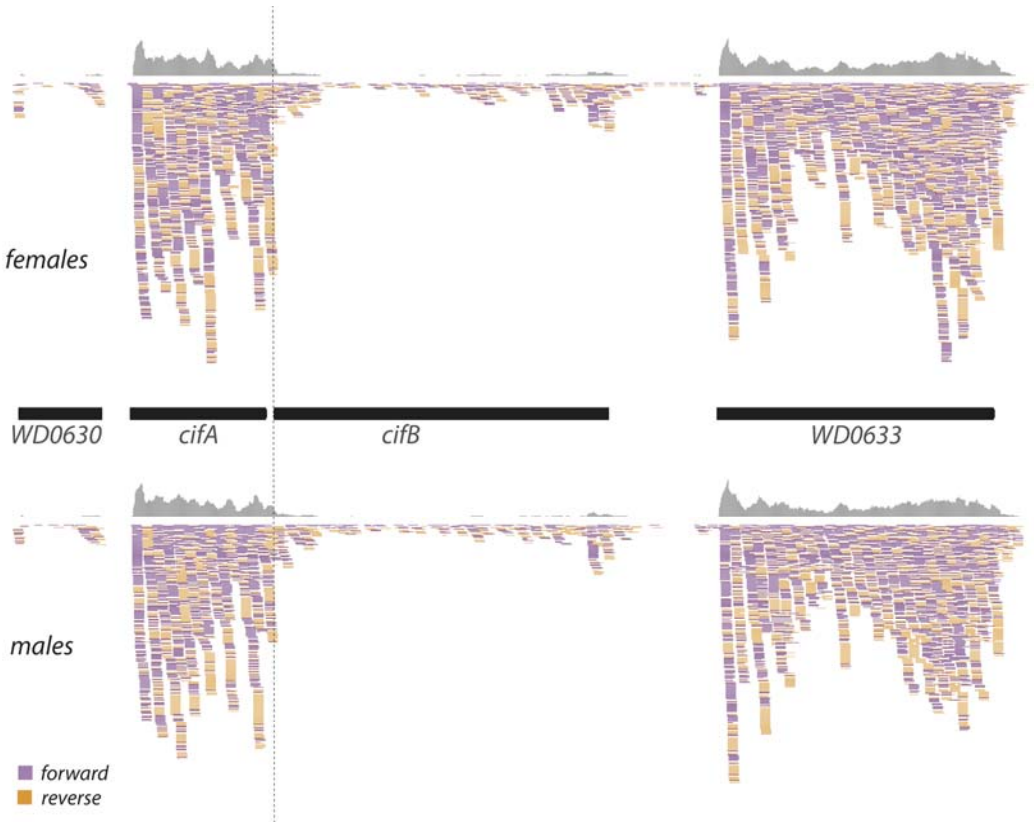

855
856

bioRxiv preprint doi: https://doi.org/10.1101/180075; this version posted August 24, 2017. The copyright holder for this preprint (which was not certified by peer review) is the author/funder. All rights reserved. No reuse allowed without permission.

857 **Figure 2**

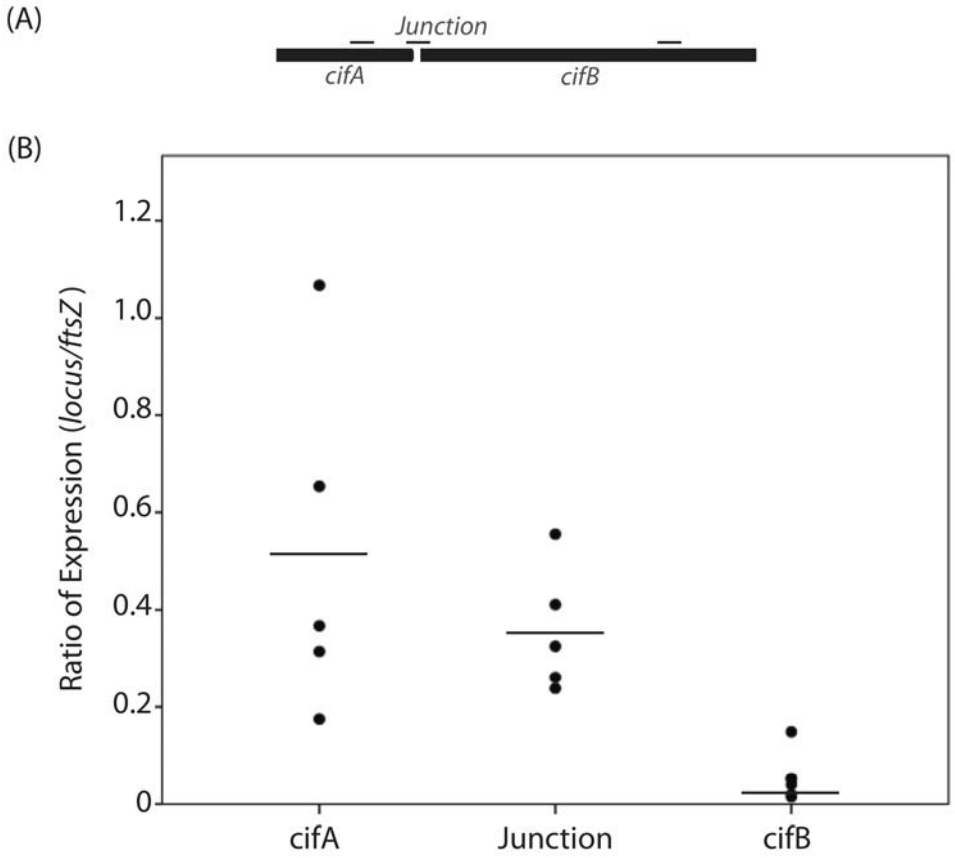

858
859

bioRxiv preprint doi: https://doi.org/10.1101/180075; this version posted August 24, 2017. The copyright holder for this preprint (which was not certified by peer review) is the author/funder. All rights reserved. No reuse allowed without permission.

Figure 3

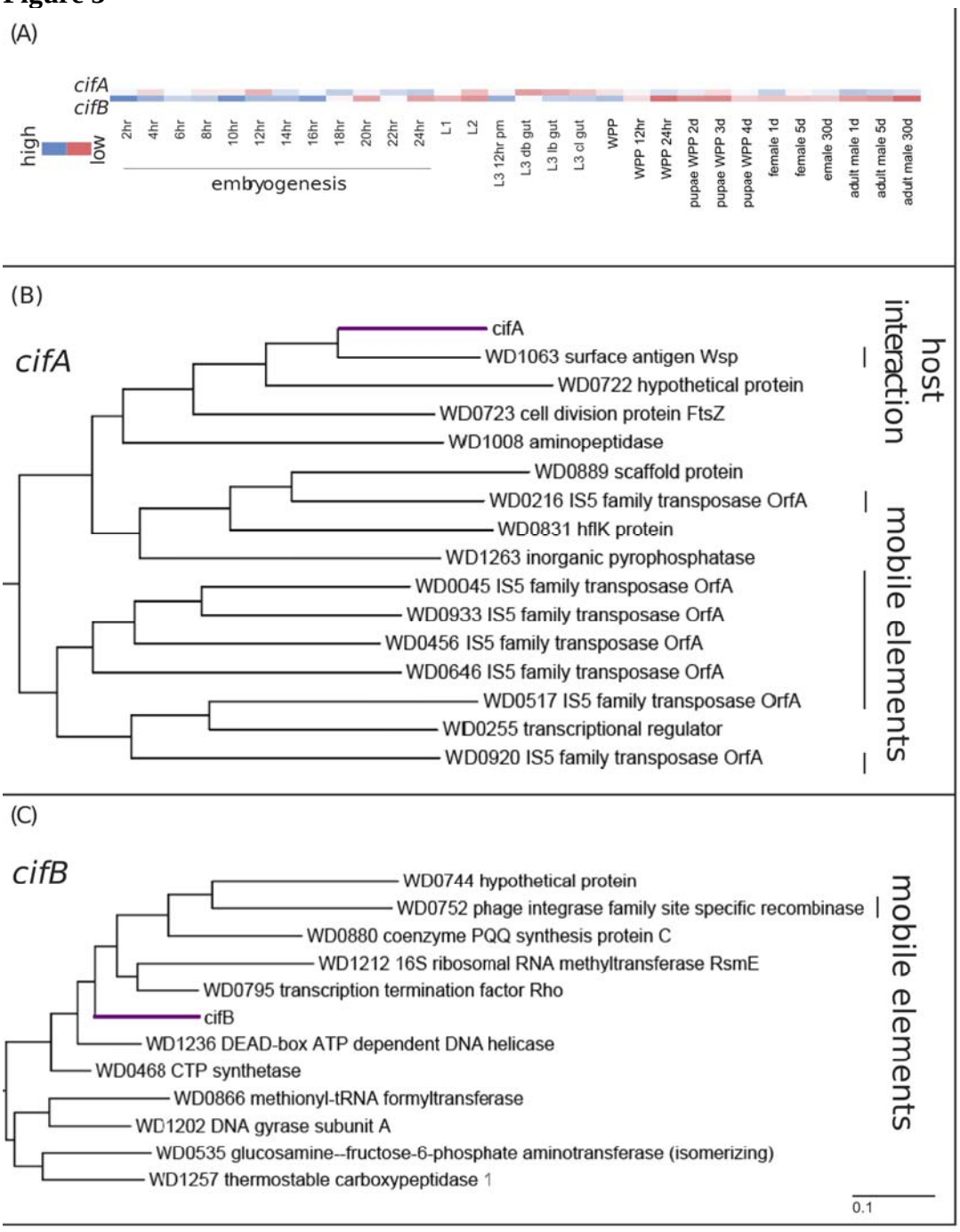

bioRxiv preprint doi: https://doi.org/10.1101/180075; this version posted August 24, 2017. The copyright holder for this preprint (which was not certified by peer review) is the author/funder. All rights reserved. No reuse allowed without permission.

Figure 4

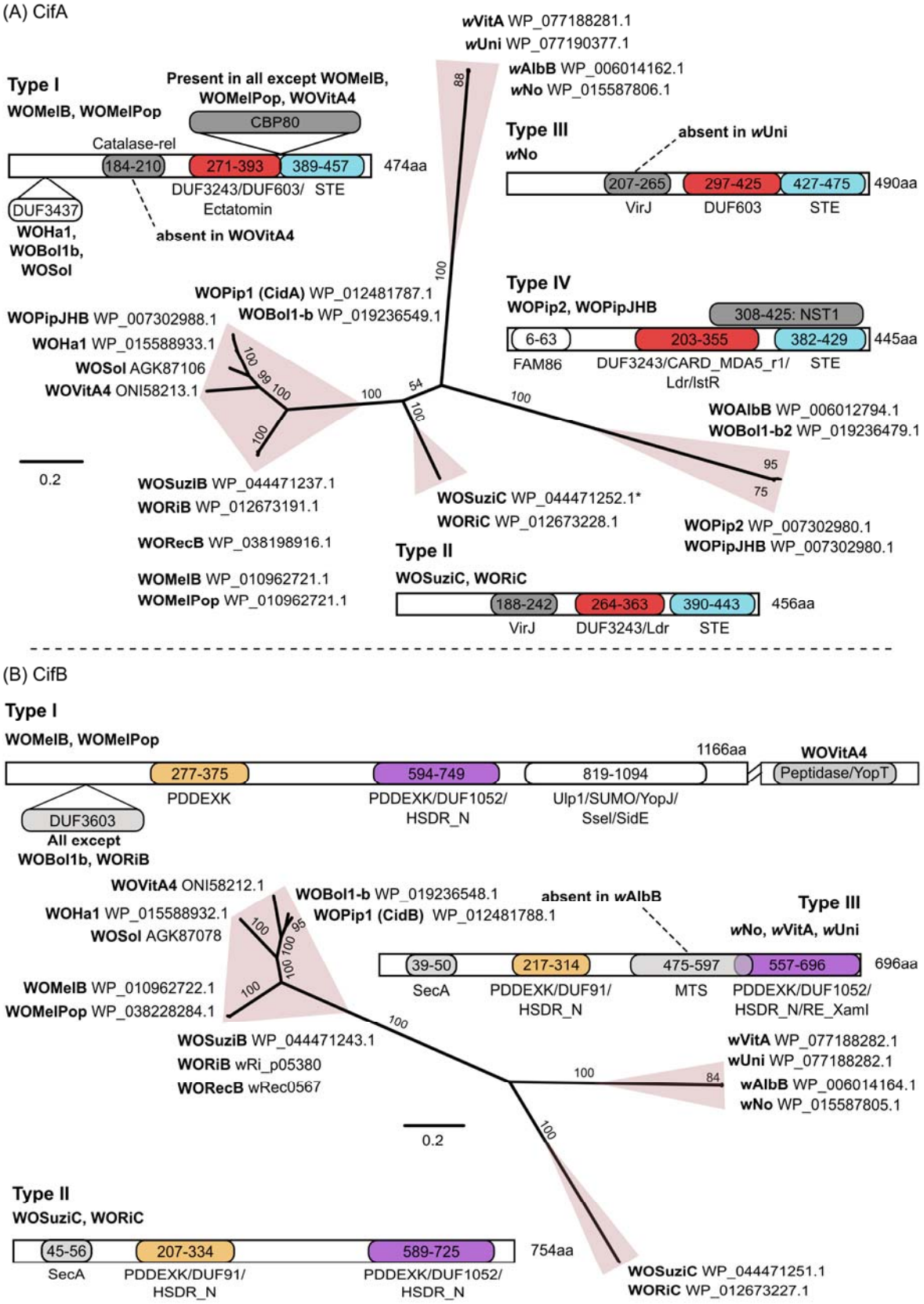

bioRxiv preprint doi: https://doi.org/10.1101/180075; this version posted August 24, 2017. The copyright holder for this preprint (which was not certified by peer review) is the author/funder. All rights reserved. No reuse allowed without permission.

865 **Figure 5**

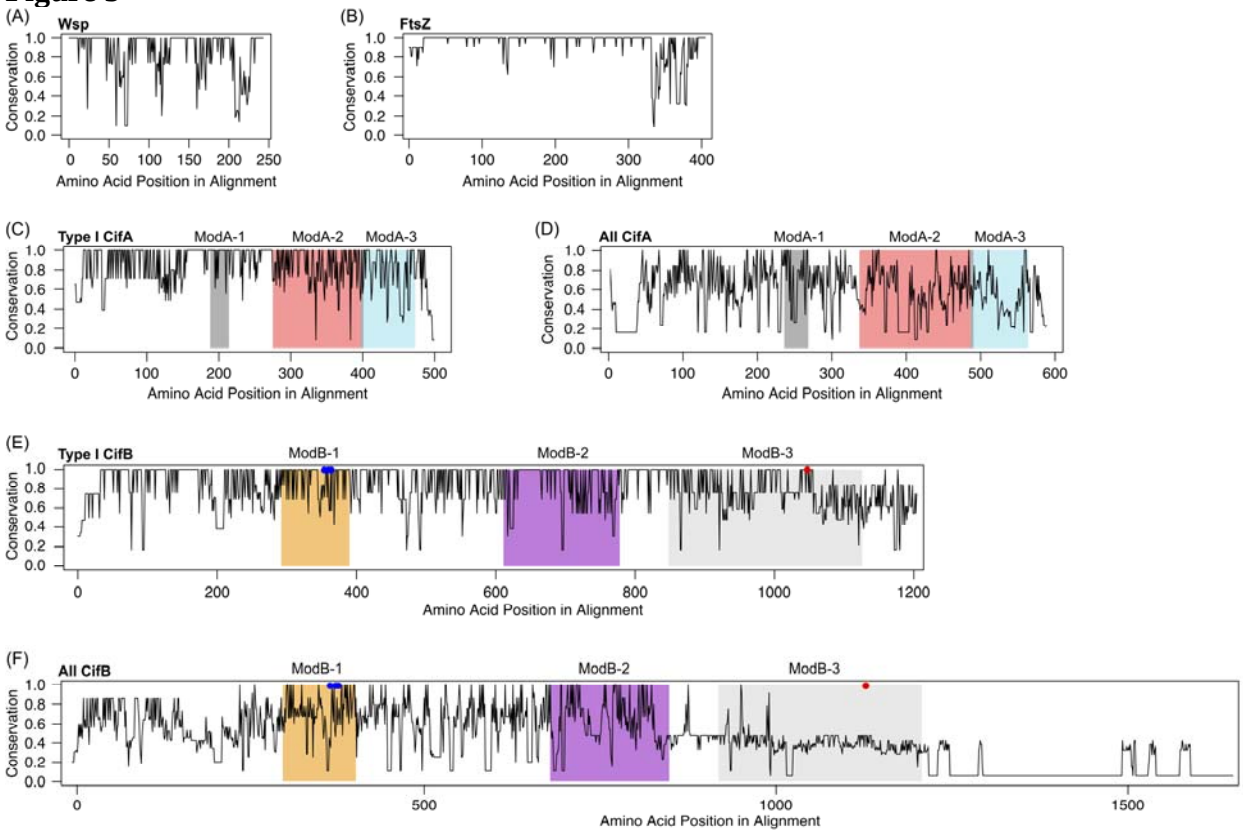

866
867

bioRxiv preprint doi: https://doi.org/10.1101/180075; this version posted August 24, 2017. The copyright holder for this preprint (which was not certified by peer review) is the author/funder. All rights reserved. No reuse allowed without permission.

868 **Figure 6**

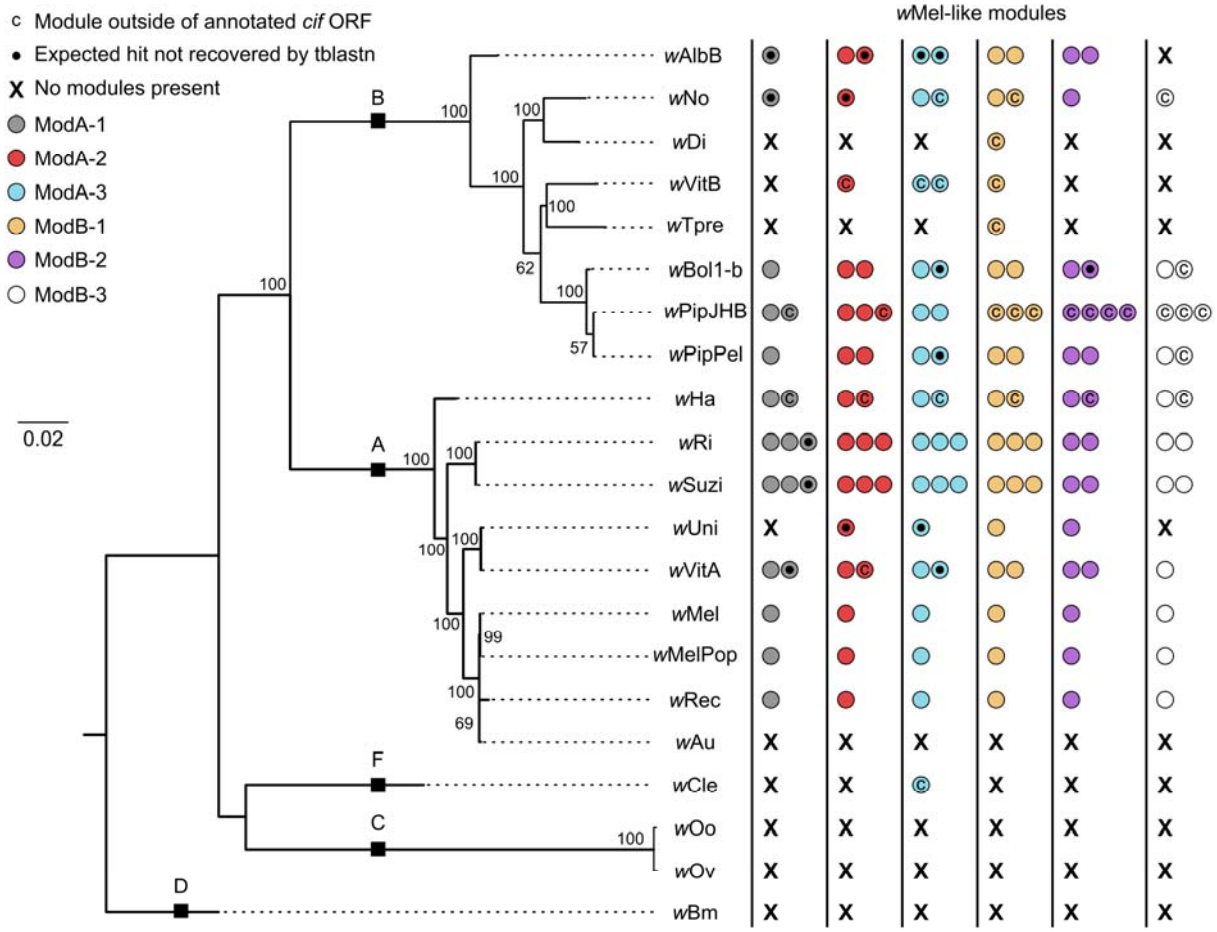

869

bioRxiv preprint doi: https://doi.org/10.1101/180075; this version posted August 24, 2017. The copyright holder for this preprint (which was not certified by peer review) is the author/funder. All rights reserved. No reuse allowed without permission.

870 **Figure legends**

871 **Fig 1. RNASeq analysis of *cifA* and *cifB* gene expression in whole adult, 1 day old female**
872 **and male *Drosophila melanogaster* flies.** Raw reads were mapped to the *w*Mel assembly (using
873 bwa) and coverage visualized using the Integrated Genomics Viewer (v2.3.77). The start of the
874 *cifB* open reading frame is denoted by a vertical, dotted line.

875

876 **Fig 2. Relative expression ratio of *cifA*, the junction between *cifA/cifB*, and *cifB* to *ftsZ*.**
877 Expression of both genes and their junction was quantified using qRT-PCR, and normalized to
878 *Wolbachia ftsZ* gene expression. *cifB* gene expression is significantly less than that of the
879 junction (t= 3.220, df=16, p=0.005) and less than *cifA* (t=-3.840, df=17, p=0.001).

880

881 **Fig 3. Gene expression of *cifA* and *cifB* during *Drosophila melanogaster* development.** A)
882 Heatmap representation of normalized transcripts per kilobase million (TPM) for both *cifA* and
883 *cifB* during *Drosophila melanogaster* development. *cifB* is highly expressed during
884 embryogenesis and downregulated after pupation while *cifA* is more highly expressed in adults
885 and pupae. Clustering of *Wolbachia* loci based on expression across fly development illustrates
886 correlated expression profiles between *w*Mel loci and *cifA* (B) or *cifB* (C). Mobile elements and
887 loci involved in host interaction (*wsp*) are indicated with vertical lines on the right side of the
888 figure.

889

890 **Fig 4. Phylogenetic relationships and representative predicted protein structure of Cif**
891 **protein types**. A) CifA and B) CifB. Alleles are in bold next to their corresponding accession
892 number, and pink shapes around branches designate monophyletic “types”. Representative

bioRxiv preprint doi: https://doi.org/10.1101/180075; this version posted August 24, 2017. The copyright holder for this preprint (which was not certified by peer review) is the author/funder. All rights reserved. No reuse allowed without permission.

893 structures are shown for each type, with the length of the protein indicated at the C-terminus.
894 Variations in within-type structure are shown. If an allele is not listed as a representative, and
895 significant structural variations are not indicated, then only the exact coordinates of the structural
896 regions differed by a few amino acids. All HHpred structural predictions are significant at a
897 corrected p-value of < 0.05, and listed in order of ascending p-value for regions with multiple
898 structural hits. Allele names use the previously described naming convention with a WO prefix
899 referring to particular phage haplotype, and the *w* prefix indicating a phage-like island (LePage,
900 et al. 2017). The N-terminus of WOSuziC (*) was translated from the end of another contig and
901 concatenated to get the full-length protein (see methods). WOMelB and WOMelPop are identical
902 at the amino acid level, as are WOPipJHB and WOPip2.
903
904 **Fig 5. Protein conservation, as determined by Shannon entropy scores**. A) Wsp (*Wolbachia*
905 surface protein), B) Cell division protein FtsZ, C) Type I CifA, D) All CifA, E) Type I CifB
906 alleles except for WOVitA4, F) All CifB alleles. Red dots in E and F indicate the ModB-3
907 catalytic residue (Beckmann, et al. 2017), unique to and completely conserved for Type I alleles.
908 Blue dots in E and F represent the (P)D-(D/E)XK motif (Kosinski, et al. 2005) present in *w*Mel.
909 We found no (P)D-(D/E)XK putative catalytic motif in the second PDDEXK-like module of
910 CifB.
911
912 **Fig 6. Presence of *w*Mel-like Cif modules across the *Wolbachia* phylogeny.** The WOMelB
913 module sequences were used to query available *Wolbachia* genomes to look for the presence of
914 Cif-like regions beyond those within the annotated Cifs (Figure 4). Colored dots correspond to
915 the structural regions delimited by HHpred, shown in Figure 4, and listed in Table 2. A "C"

bioRxiv preprint doi: https://doi.org/10.1101/180075; this version posted August 24, 2017. The copyright holder for this preprint (which was not certified by peer review) is the author/funder. All rights reserved. No reuse allowed without permission.

916 within a dot indicates the presence of a module outside of annotated *cif* open reading frames
917 (Figure 4 and Supplemental Figures S2 and S3). The black dot indicates a module annotated by
918 HHpred, but not identified by tblastn due to divergence from the WOMelB module. Black boxes
919 labeled with uppercase letters indicate branches leading to *Wolbachia* Supergroups. Dotted lines
920 on the phylogeny lead to taxon names and are not included in the branch length.